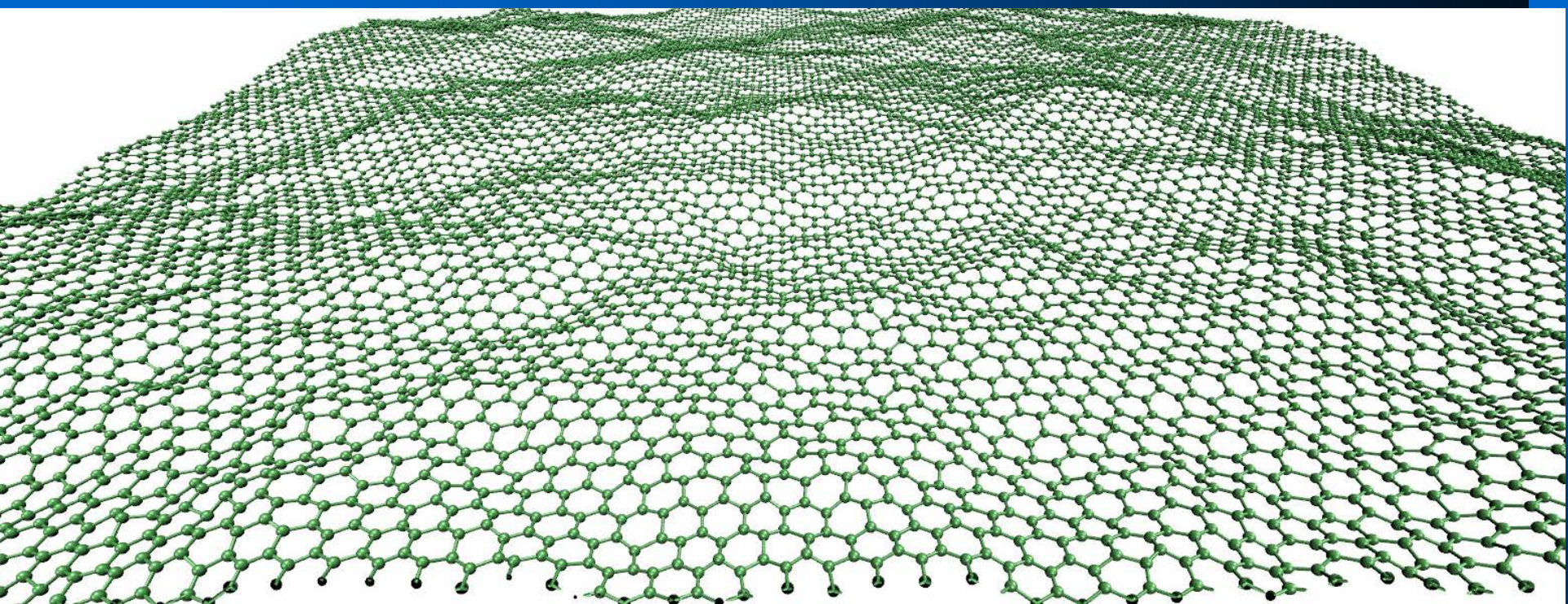


Theory of graphene: CERN on the desk

Mikhail Katsnelson



<http://www.ru.nl/tcm/>



Instead of epigraph

You can get much further with a *kind word* and
a *gun* than you can with a *kind word* alone
(Al Capone)



You can get much further with an insight from
experiment and mathematics than you can
with mathematics alone

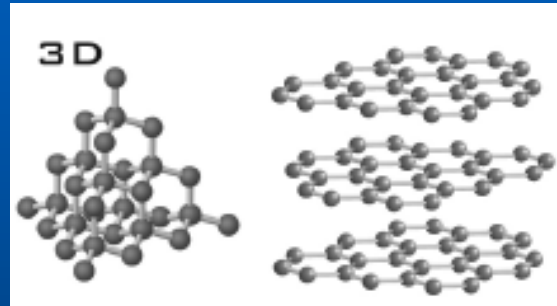
Carbon, an elemental solid



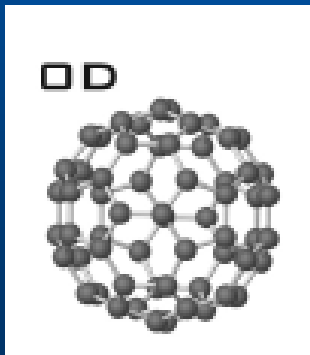
Diamond



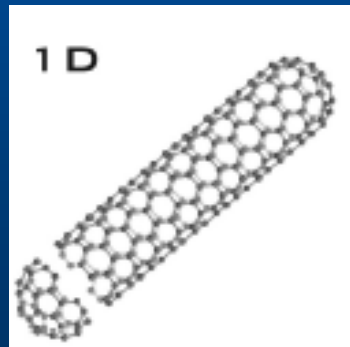
Graphite



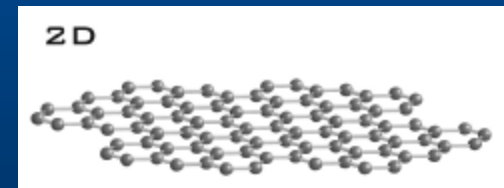
Crystal lattices



Fullerenes

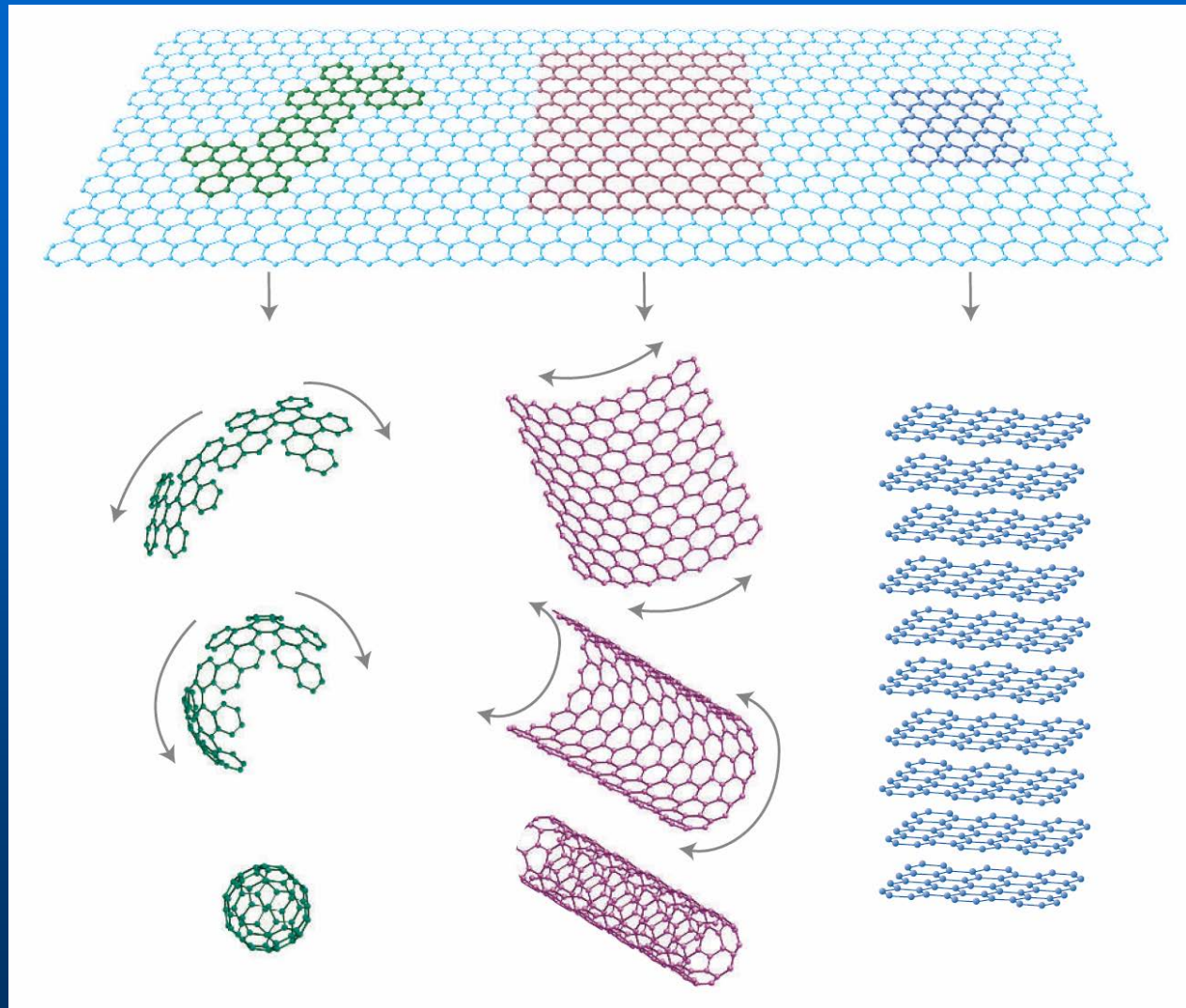


Nanotubes



Graphene

Mother of all graphitic forms



Fullerenes

Nanotubes

Graphite

Why graphene is interesting?

Till 2004: a way to understand graphite, nanotubes, fullerenes + theoretical interest

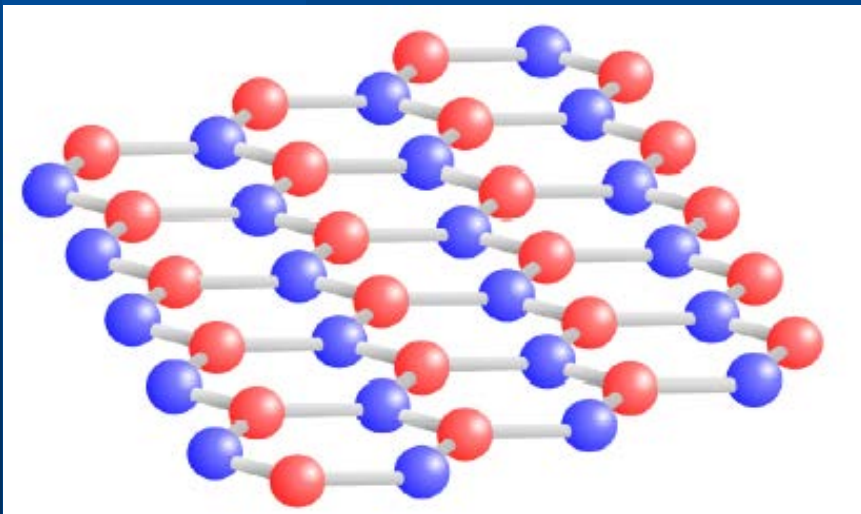
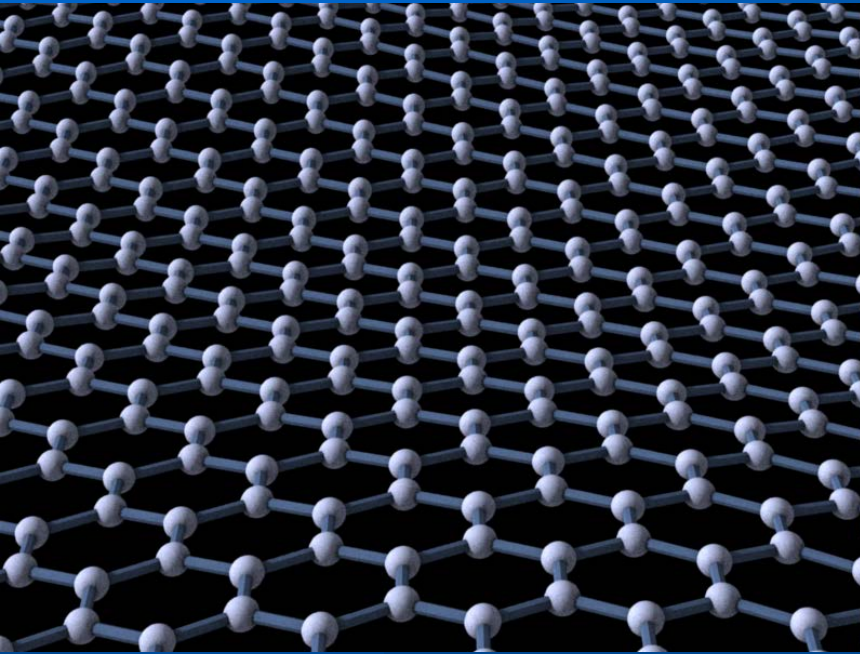
(Dirac point Wallace 1947, McClure 1956...)

Do we theoreticians need experimentalists?! – Yes!!!

(Klein tunneling, supercritical charge, ripples, new wave equation – bilayer, new type of transport...)

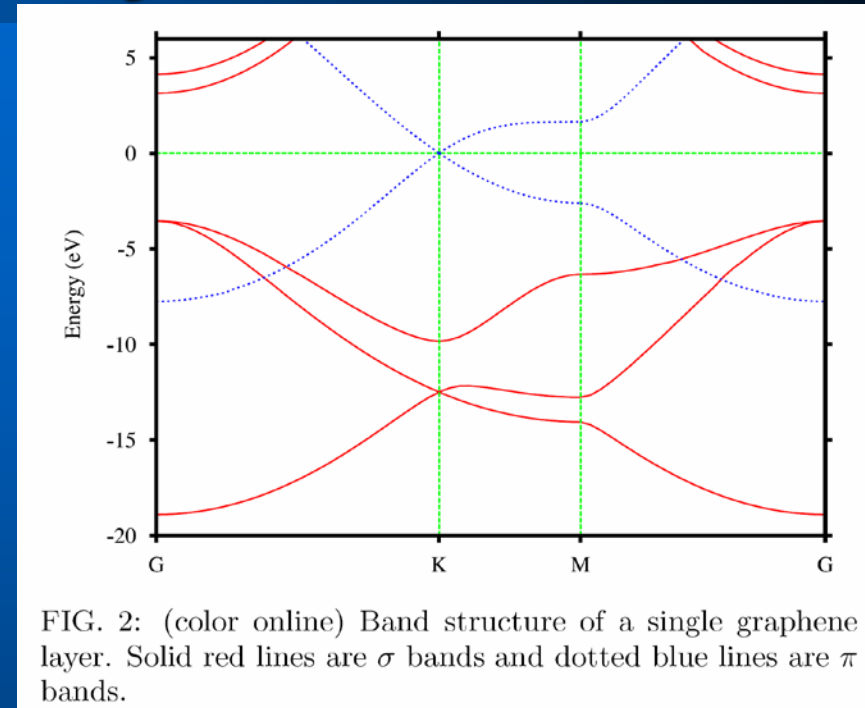
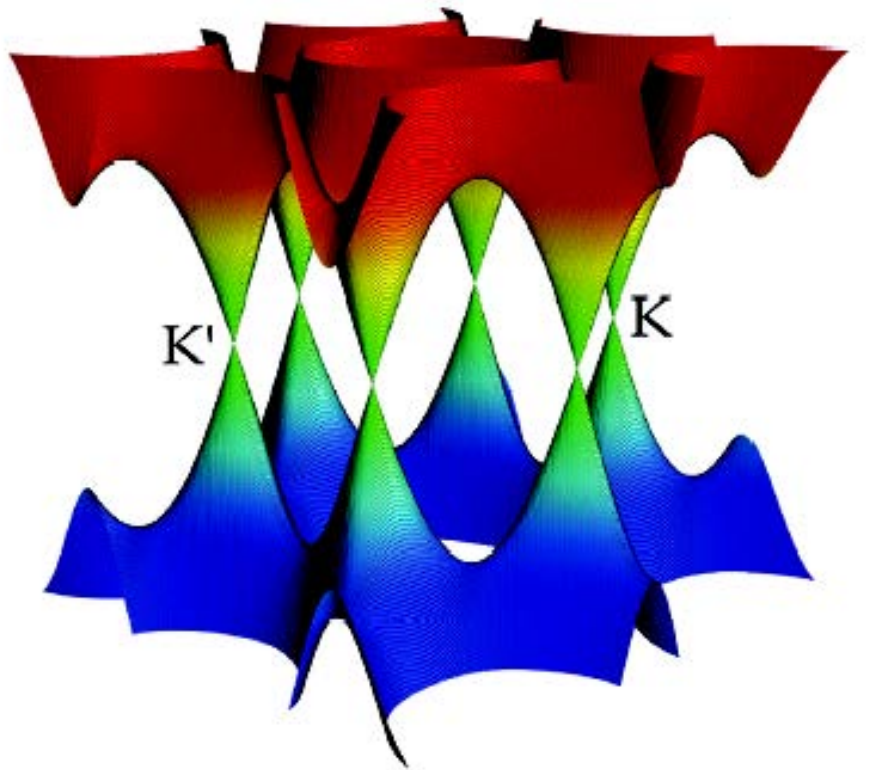
1. *Applications (modern electronics is 2D, bulk is ballast)*
2. *Prototype membrane (new drosophila for 2D statistical mechanics)*
3. *CERN on the desk (mimic high energy physics)*

Honeycomb lattice



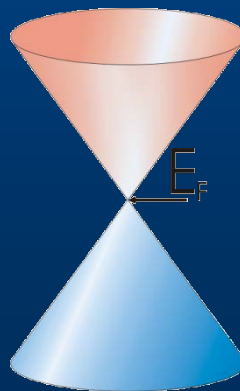
Two equivalent sublattices,
A and B (pseudospin)

Massless Dirac fermions



sp^2 hybridization, π bands crossing the neutrality point

Massless relativistic particles (light cones)

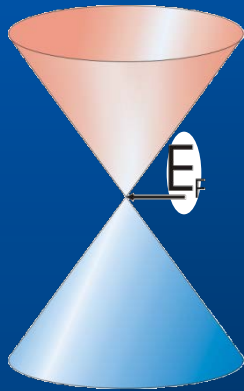


Neglecting intervalley scattering:
massless Dirac fermions

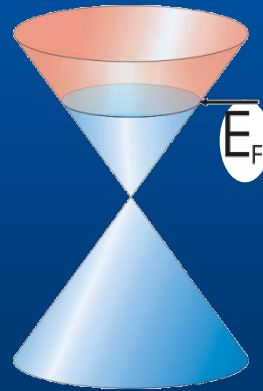
Symmetry protected (T and I)

Massless Dirac fermions II

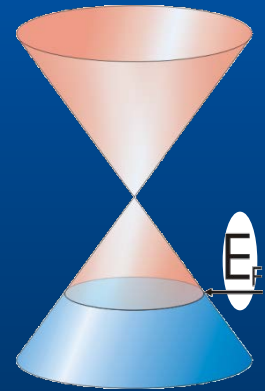
Spectrum near K (K') points is linear.
Conical cross-points: provided by symmetry and thus robust property



Undoped



Electron



Hole

Massless Dirac fermions III

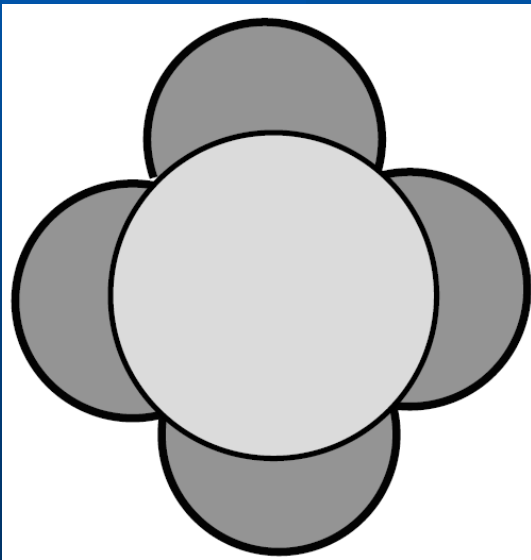
If Umklapp-processes K-K' are neglected:
2D Dirac massless fermions with the Hamiltonian

$$H = -i\hbar c^* \begin{pmatrix} 0 & \frac{\partial}{\partial x} - i \frac{\partial}{\partial y} \\ \frac{\partial}{\partial x} + i \frac{\partial}{\partial y} & 0 \end{pmatrix} \quad \hbar c^* = \frac{\sqrt{3}}{2} \gamma_0 a$$

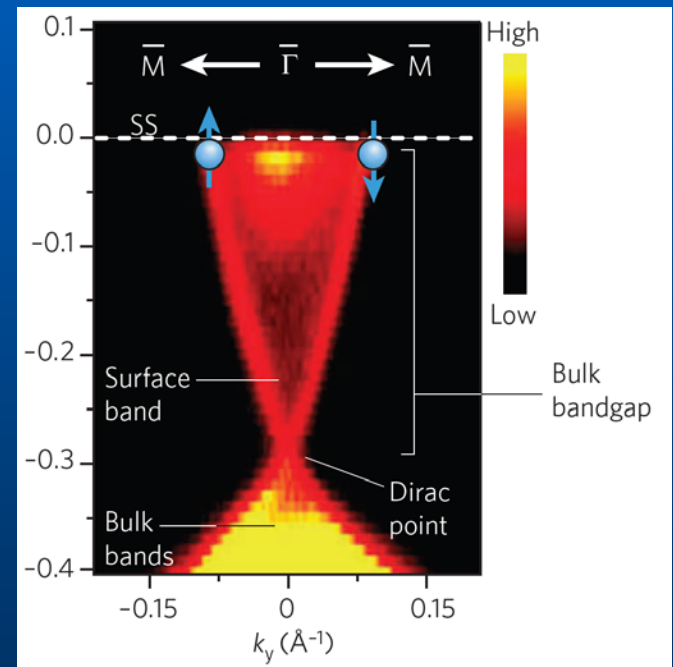
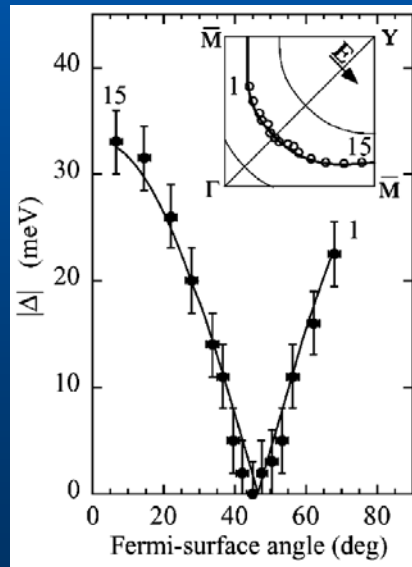
“Spin indices” label sublattices *A* and *B*
rather than real spin

Massless Dirac fermions in condensed matter physics

1. d-wave superconductors
2. Vortices in superconductors and in superfluid helium-3
3. Topological insulators
4. Graphene

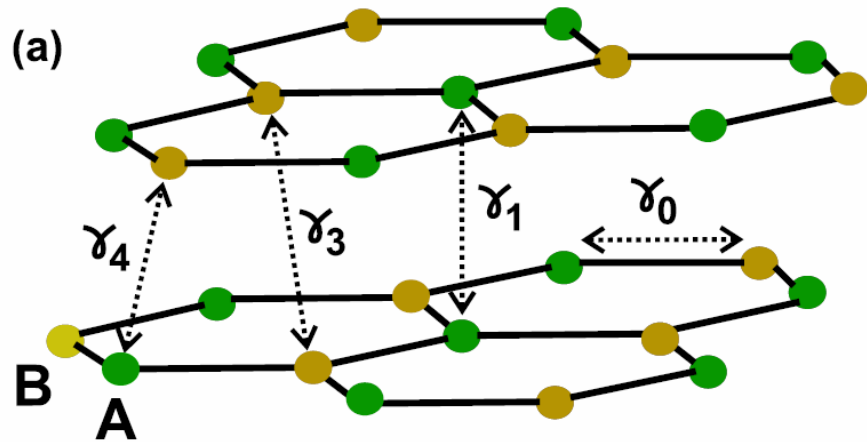


Gap in high-Tc cuprates



Electronic structure on surface of Bi_2Se_3

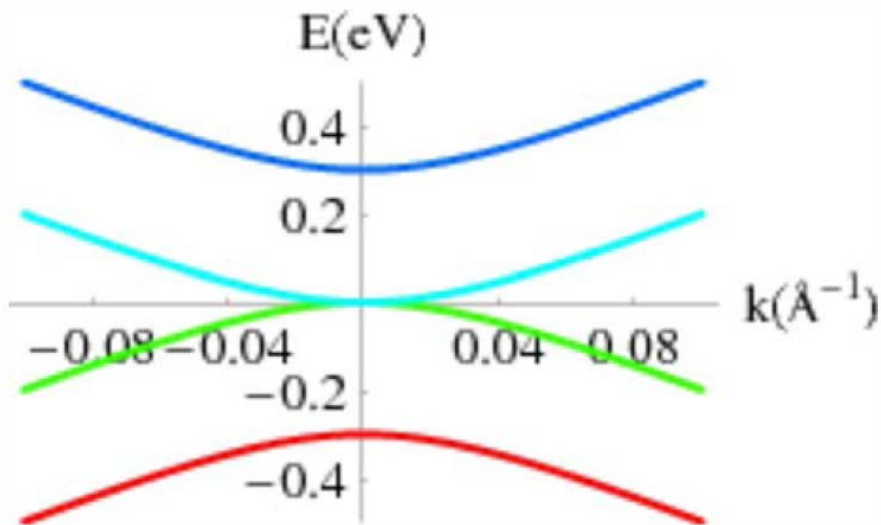
Bilayer graphene – TB description



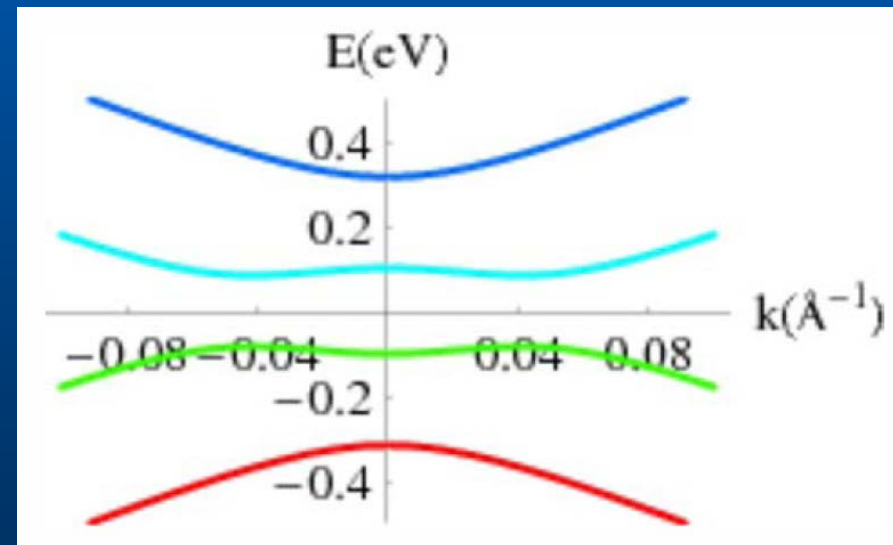
$$H = \begin{pmatrix} 0 & -(p_x - ip_y)^2/2m \\ -(p_x + ip_y)^2/2m & 0 \end{pmatrix}$$

$$m^* \approx 0.028m_e$$

(neglecting γ_3)



Gapless, parabolic



Electric field perp. layers

Bilayer graphene II

Trigonal warping, many-body effects and spectrum reconstruction at small energies

Single-particle Hamiltonian:

$$\hat{H}_K = \begin{pmatrix} 0 & \frac{(\hat{p}_x - i\hat{p}_y)^2}{2m^*} + \frac{3\gamma_3 a}{\hbar} (\hat{p}_x + i\hat{p}_y) \\ \frac{(\hat{p}_x + i\hat{p}_y)^2}{2m^*} + \frac{3\gamma_3 a}{\hbar} (\hat{p}_x - i\hat{p}_y) & 0 \end{pmatrix}$$



Interaction-Driven Spectrum Reconstruction in Bilayer Graphene

A. S. Mayorov,¹ D. C. Elias,¹ M. Mucha-Kruczynski,² R. V. Gorbachev,³ T. Tudorovskiy,⁴
A. Zhukov,³ S. V. Morozov,⁵ M. I. Katsnelson,⁴ V. I. Fal'ko,² A. K. Geim,³ K. S. Novoselov^{1*}

12 AUGUST 2011 VOL 333 SCIENCE

Outline

Graphene in magnetic field: a physical realization of index theorem

Minimal conductivity problem and transport via evanescent waves

Klein tunneling and inhomogeneities

Chiral tunneling - bilayer

Relativistic collapse for supercritical charges

Pseudomagnetic gauge field and “strain engineering”

Effective Hamiltonian in magnetic field: Peierls

$$H = \frac{\hat{\pi}^2}{2m} + V(\vec{r})$$

$$\hat{\pi} = \hat{\vec{p}} - \frac{e}{c} \vec{A},$$

$$\vec{p} = -i\hbar \vec{\nabla}$$

$$\vec{B} = \vec{\nabla} \times \vec{A},$$

$V(\vec{r})$ is a periodic crystal potential

$$[\hat{\pi}_x, \hat{\pi}_y] = -[\hat{\pi}_y, \hat{\pi}_x] = \frac{ie}{\hbar c} B$$

Exact formulation

Simplifications:

$$l_B \gg a$$

up to 10,000 T – OK!

$$l_B = \sqrt{\frac{\hbar c}{|e|B}}$$

magnetic length

Effective Hamiltonian II

Single band model (neglecting magnetic breakdown) – fine for π -band in graphene, no restrictions, actually

$$\hat{H}_{ef} = t(\hat{\vec{\pi}})$$

$$t(\hat{\vec{\pi}})\psi = E\psi$$

Bosonic operators

$$\hat{\pi}_- = \hat{\pi}_x - i\hat{\pi}_y = \sqrt{\frac{2|e|\hbar B}{c}}\hat{b},$$

$$\hat{\pi}_+ = \hat{\pi}_x + i\hat{\pi}_y = \sqrt{\frac{2|e|\hbar B}{c}}\hat{b}^+$$

$$[\hat{b}, \hat{b}^+] = 1$$

Dirac electrons

$$\hat{H} = v \begin{pmatrix} 0 & \hat{\pi}_- \\ \hat{\pi}_+ & 0 \end{pmatrix} = \sqrt{\frac{2|e|\hbar B v^2}{c}} \begin{pmatrix} 0 & \hat{b} \\ \hat{b}^+ & 0 \end{pmatrix}$$

Solution

$$\begin{aligned}\hat{b}\psi_2 &= \varepsilon\psi_1 \\ \hat{b}^+\psi_1 &= \varepsilon\psi_2\end{aligned}$$

$$E = \sqrt{\frac{2|e|\hbar B v^2}{c}} \varepsilon \equiv \frac{\sqrt{2}\hbar v}{l_B} \varepsilon$$

Zero-energy solution:

$$\psi_1 = 0$$

$$\psi_2 \equiv |0\rangle$$

$$b|0\rangle = 0$$

Complete spectrum:

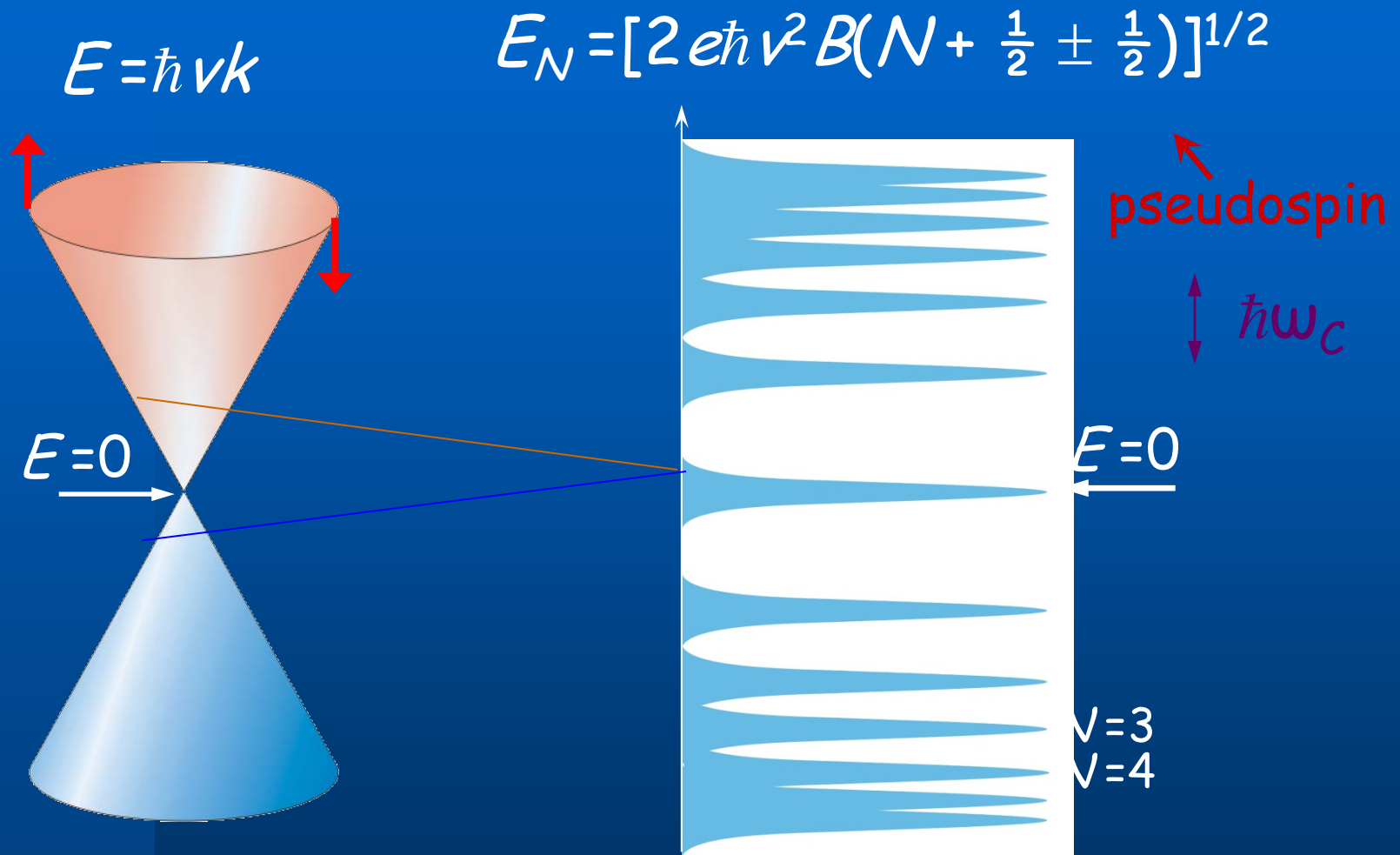
$$\hat{b}^+\hat{b}\psi_2 = \varepsilon^2\psi_2$$

$$\varepsilon_v^2 = v = 0, 1, 2, \dots$$

$$E_v^{(\pm)} = \pm \hbar \omega_c \sqrt{v}$$

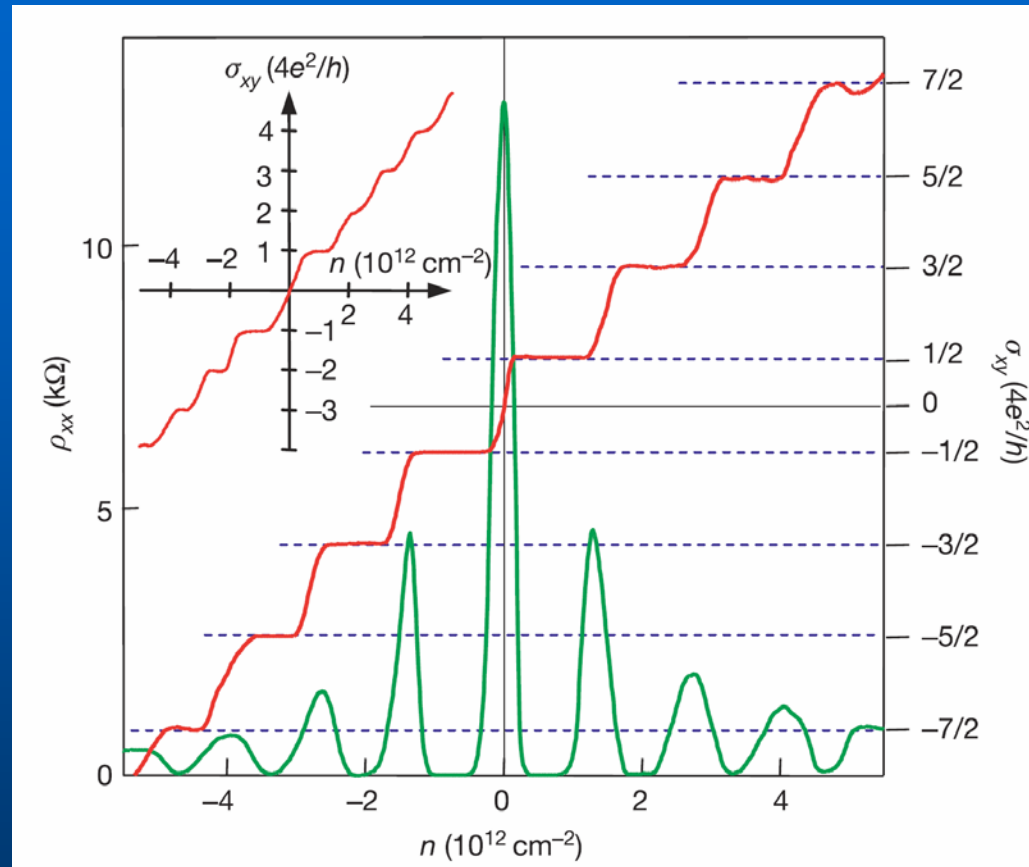
$$\hbar \omega_c = \frac{\sqrt{2}\hbar v}{l_B} = \sqrt{\frac{2\hbar|e|Bv^2}{c}}$$

Anomalous Quantum Hall Effect



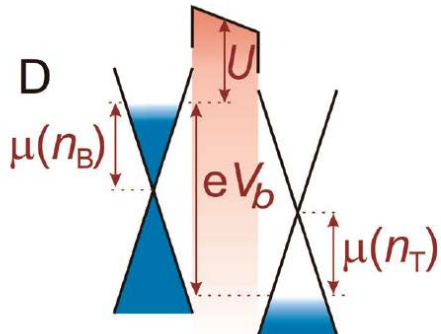
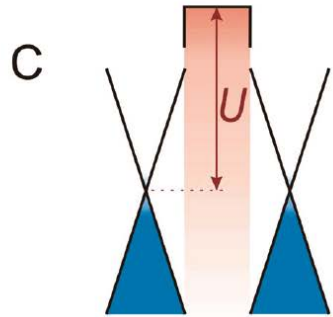
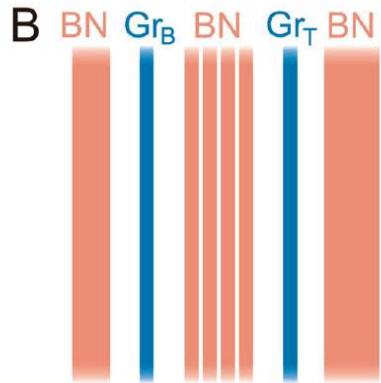
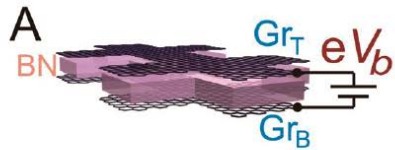
The lowest Landau level is *at ZERO energy* and shared equally by electrons and holes (McClure 1956)

Anomalous QHE in single-layer graphene



Single-layer: half-integer quantization since zero-energy Landau level is equally shared by electrons and holes (Novoselov et al 2005, Zhang et al 2005)

Quantum capacitance



$$eV_b = eF_b d - \mu(n_T) + \mu(n_B)$$

Assuming for simplicity $\mu(-n) = -\mu(n)$

$$\frac{e^2 d}{\epsilon_0 \epsilon_r} n_T + \mu(n_T) + \mu\left(n_T + \frac{\epsilon_0 \epsilon_r F_g}{e}\right) + eV_b$$

For small bias:

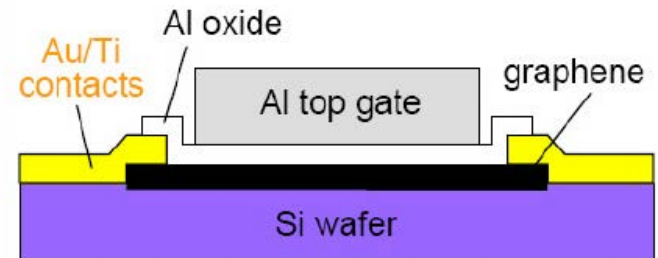
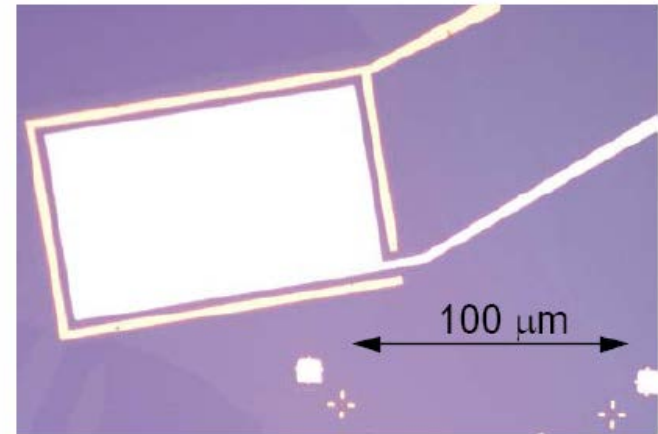
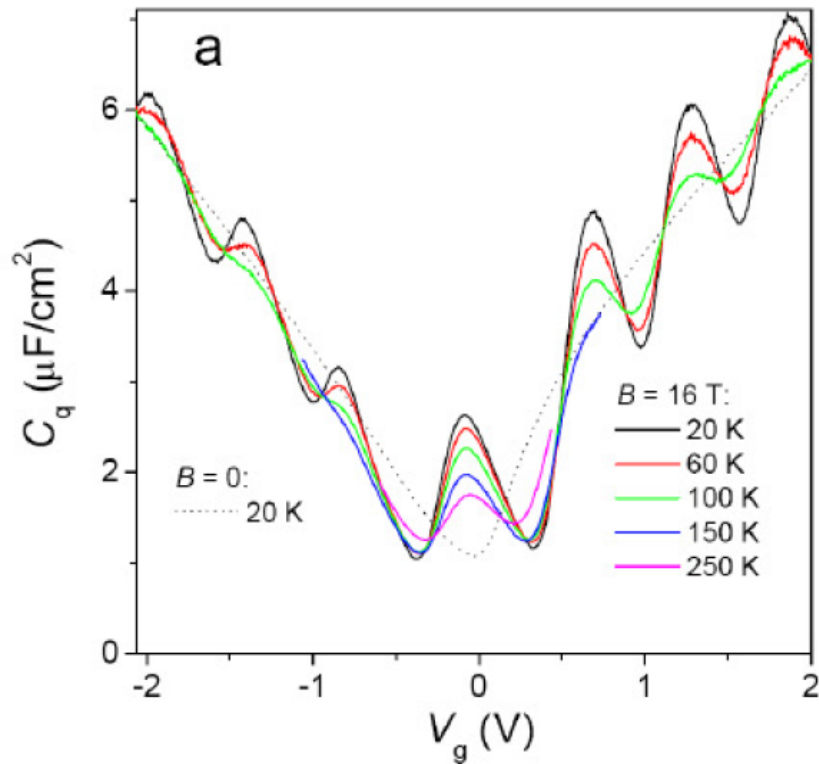
$$1/C = 1/C_G + 1/C_Q,$$

G means “geometrical”

$$C_Q = Se^2 \, dn/d\mu.$$

Quantum capacitance II

Ponomarenko et al, PRL 2010



Quantum capacitance III

Yu et al, PNAS 2013

Graphene on hBN: one can see many-body effects etc.

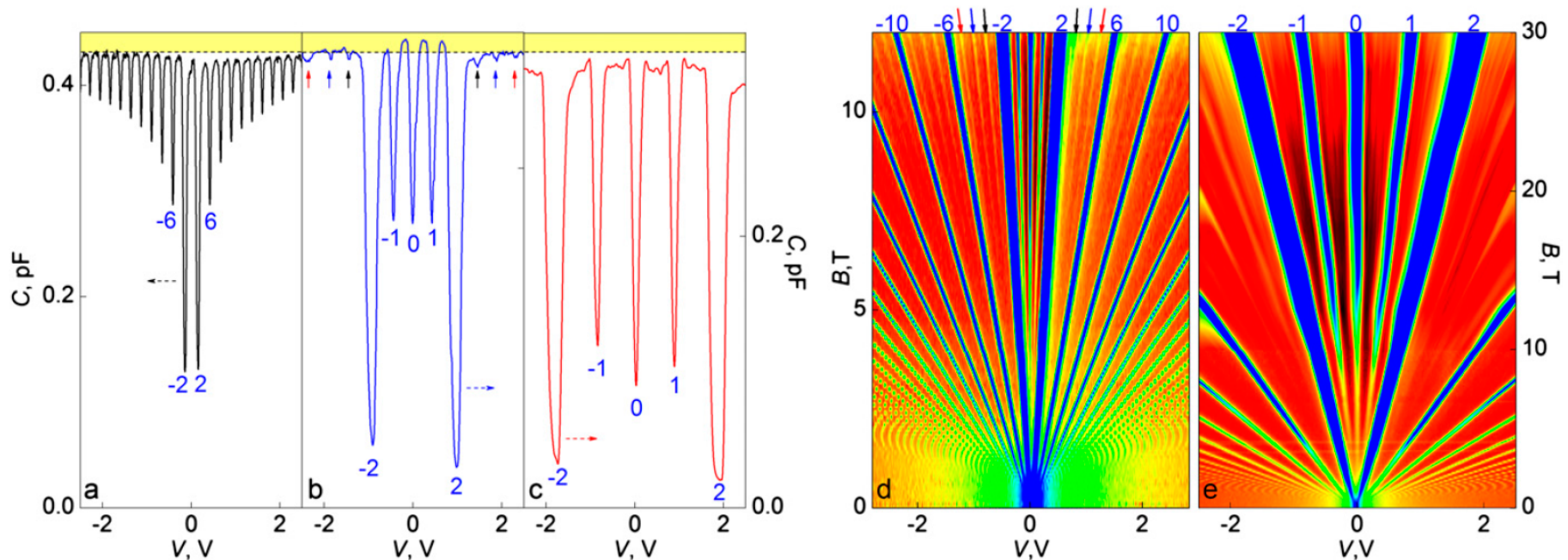


Fig. 3. Graphene capacitors in quantizing fields. (A–C) Examples of graphene capacitance for $B = 3, 15$, and 30 T, respectively. Blue numbers are ν for the corresponding minima. The arrows in B mark $\nu = \pm 3$ (black arrows), ± 4 (blue) and ± 5 (red). The dashed line indicates $C_G = 0.433 \pm 0.002$ pF (for a device shown in A) and 0.335 ± 0.002 pF (for a device shown in B and C). The 15-T curve reveals that the total capacitance becomes higher than the geometrical one at ν around $\pm 1/2$ and $\pm 3/2$, indicating a negative contribution from C_Q , that is, negative compressibility. (D) Two-dimensional map of differential capacitance as a function of B and V for the same device as in A. Color scale is 0.37 pF to C_G (blue to green to red) and C_G to 0.454 pF (red to black). Numbers and arrows are as in B. (E) Two-dimensional map in B up to 30 T for the device in B and C. Scale: 0.23 pF to C_G (blue to green to red) and C_G to 0.349 pF (red to black). The dark regions (D and E) correspond to negative C_Q .

Semiclassics

$$S(E_\nu) = \frac{2\pi|e|B}{\hbar c} \left(\nu + \frac{1}{2} - \frac{\gamma}{2\pi} \right)$$

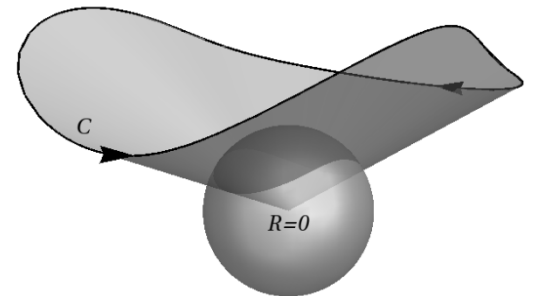
$\nu = 0, 1, 2, \dots$ γ is the Berry phase

$$\gamma_n(C) = - \int d\vec{S} \vec{V}_n(\vec{k})$$

$$\vec{V}_n = \text{Im} \sum_{m \neq n} \frac{\langle n | \vec{\nabla}_{\vec{k}} \hat{H}_{ef} | m \rangle \times \langle m | \vec{\nabla}_{\vec{k}} \hat{H}_{ef} | n \rangle}{(E_m - E_n)^2}$$

$$\hat{H}_{ef} = \frac{1}{2} \vec{R}(\vec{k}) \vec{\sigma}$$

$$\gamma_{\pm}(C) = \mp \frac{1}{2} \Omega(C)$$



2D Dirac: $\gamma = \pi$

Half-integer quantum Hall effect and “index theorem”

Atiyah-Singer index theorem: number of chiral
modes with zero energy for massless Dirac
fermions with gauge fields

Simplest case: 2D, electromagnetic field

$$N_+ - N_- = \phi / \phi_0$$

(magnetic flux in units of the flux quantum)

Magnetic field can be inhomogeneous!!!

Anomalous QHE for bilayer graphene

Low-energy description:
Massive chiral fermions

$$H = \begin{pmatrix} 0 & -(p_x - ip_y)^2/2m \\ -(p_x + ip_y)^2/2m & 0 \end{pmatrix}$$

Homogeneous magnetic
Field ($\nu = 0, 1, 2, \dots$)

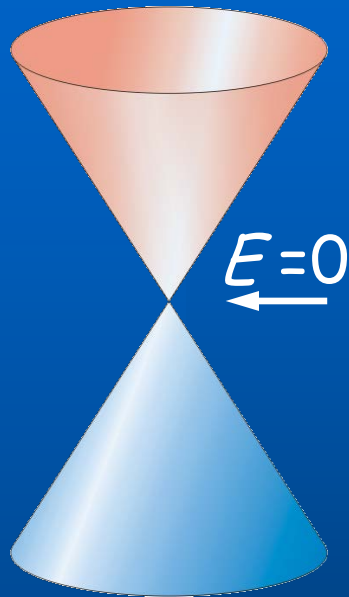
$$E_\nu \propto \sqrt{\nu(\nu - 1)}$$

Index theorem for
bilayer graphene (MIK and
M. Prokhorova, PR B 2008)

$$N_+ - N_- = 2\phi / \phi_0$$

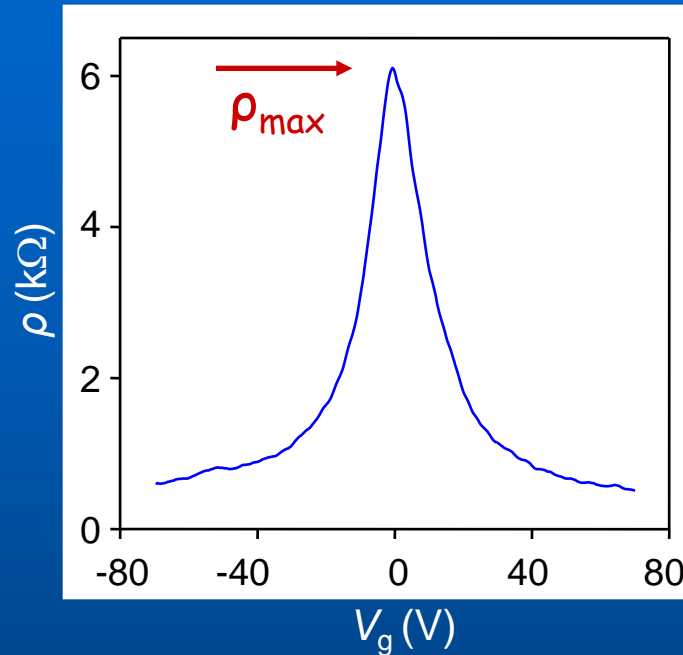
Anomalous QHE in inhomogeneous field!

Quantum-Limited Resistivity

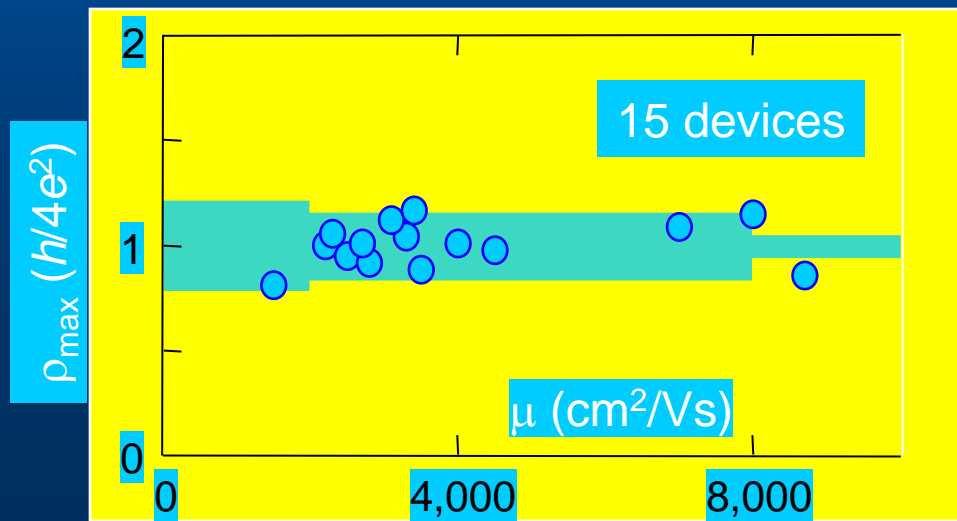


zero-gap
semiconductor

Novoselov et al,
Nature 2005



no temperature
dependence
in the peak
between 3 and 80K



Transport via evanescent waves

MIK, EPJ B 51, 157 (2006)

Conductance = $e^2/h \text{ Tr } T$ per valley per spin

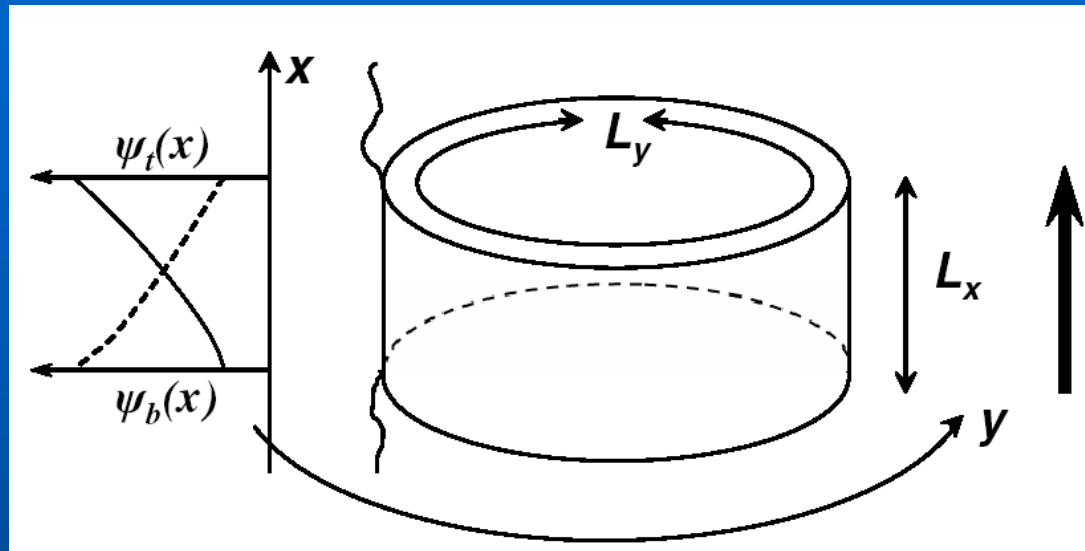
T is the transmission probability matrix

The wave functions of massless
Dirac fermions at zero energy:

$$\left(\frac{\partial}{\partial x} \pm i \frac{\partial}{\partial y} \right) \psi_{\pm}(x, y) = 0 \quad \psi_{\pm}(x, y) = f(x \pm iy) \quad \forall f$$

Boundary conditions determine the functions f

Transport via evanescent waves II



$$\psi_{\pm}(x, y) = \exp\left[\frac{2\pi n}{L_y}(x \pm iy)\right] \quad n = 0, \pm 1, \pm 2, \dots$$

$f(y+L_y) = f(y)$ Edge states near the top and bottom of the sample

New type of electron transport: via evanescent waves – different from both ballistic and diffusive

Transport via evanescent waves III

Leads from doped graphene

$$T_n = |t(k_y)|^2 = \frac{\cos^2 \phi}{\cosh^2(k_y L_x) - \sin^2 \phi}$$

$$\sin \phi = k_y / k_F$$

$$TrT = \sum_{n=-\infty}^{\infty} \frac{1}{\cosh^2(k_y L_x)} \simeq \frac{L_y}{\pi L_x}$$

Conductivity per channel: $e^2 / (\pi h)$

Seems to be in agreement with the latest experiments

Transport via evanescent waves IV

Recent experiment

In very clean samples min conductivity is close to theor. prediction

How Close Can One Approach the Dirac Point in Graphene Experimentally? *Nano Lett.* 2012, 12, 4629–4634

Alexander S. Mayorov,^{*,†} Daniel C. Elias,[†] Ivan S. Mukhin,[‡] Sergey V. Morozov,[§] Leonid A. Ponomarenko,[†] Kostya S. Novoselov,[†] A. K. Geim,^{†,‡} and Roman V. Gorbachev^{†,‡}

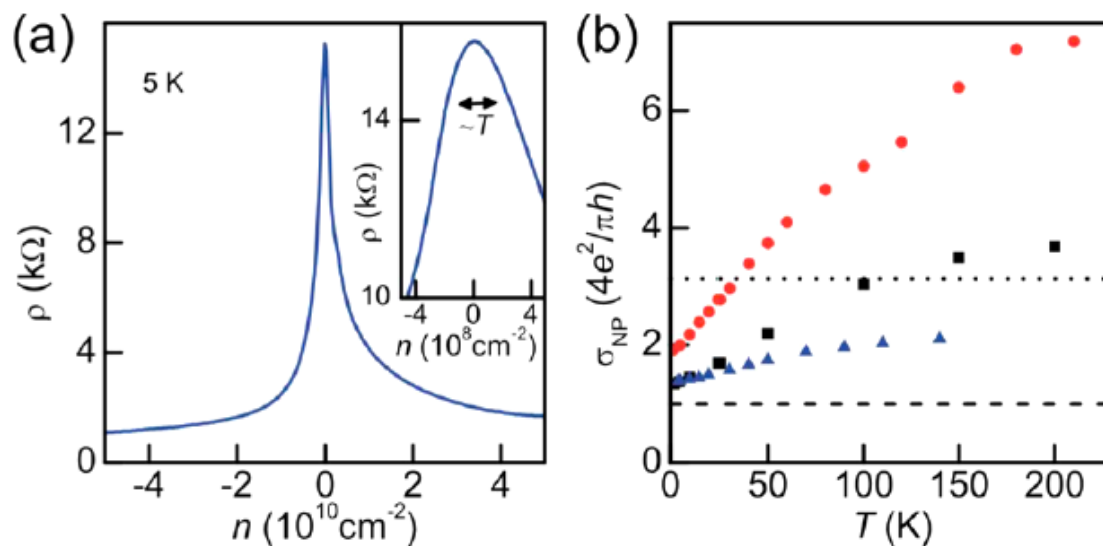


Figure 3. Height and broadening of the resistivity peak. (a) $\rho(n)$ for one of our devices. Inset: thermal smearing of the tip. (b) T dependence of σ at the NP for three devices. The dashed line indicates the ballistic limit; the dotted one is $4e^2/h$. For the sake of generality, no contact resistance is subtracted, which would result in slightly higher values of σ_{NP} .

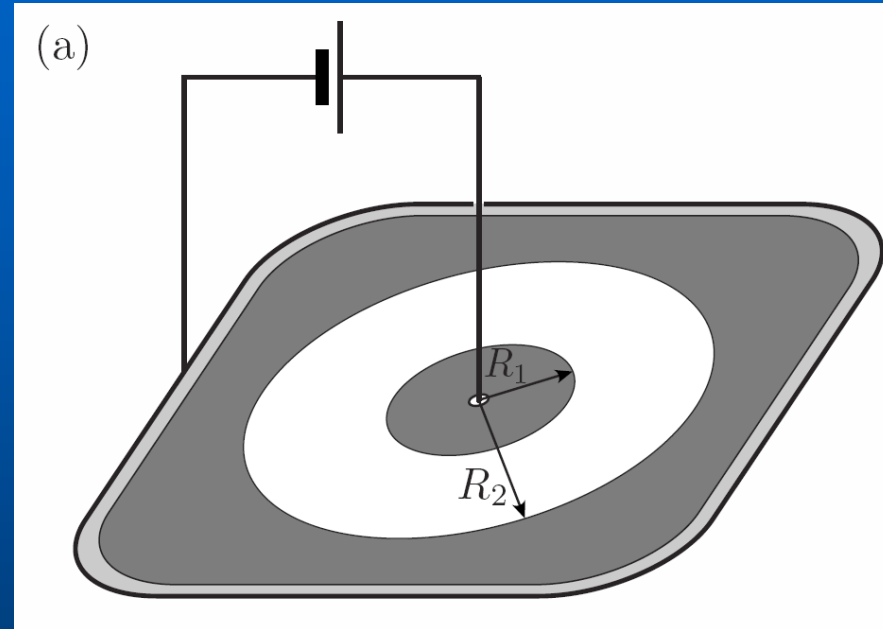
Other geometries by conformal mapping

(MIK and Guinea, PR B 2008; Rycerz, Recher and Wimmer, PR B 2010)

$$T_j = \frac{1}{\cosh^2[gj \ln \Lambda\{z(w)\}]}$$

$$j = \pm \frac{1}{2}, \pm \frac{3}{2}, \dots$$

Λ transforms the region to circular ring (Corbino geometry)



$$G_{\text{diff}} = \frac{2\pi\sigma_0}{\ln(R_2/R_1)}$$

Aharonov-Bohm effect at zero doping

MIK, EPL 89, 17001 (2009)

Magnetic flux tube within the ring

$$G = G_0 \left[1 - \frac{4\pi^2}{\ln(R_2/R_1)} \exp\left(-\frac{\pi^2}{\ln(R_2/R_1)}\right) \cos\left(\frac{e\Phi}{\hbar c}\right) \right]$$

General shape (topologically equivalent to rings)

$$G = G_0 \left[1 - \frac{4\pi^2}{\beta} \exp(-\pi^2/\beta) \cos\left(\frac{e\Phi}{\hbar c}\right) \right]$$

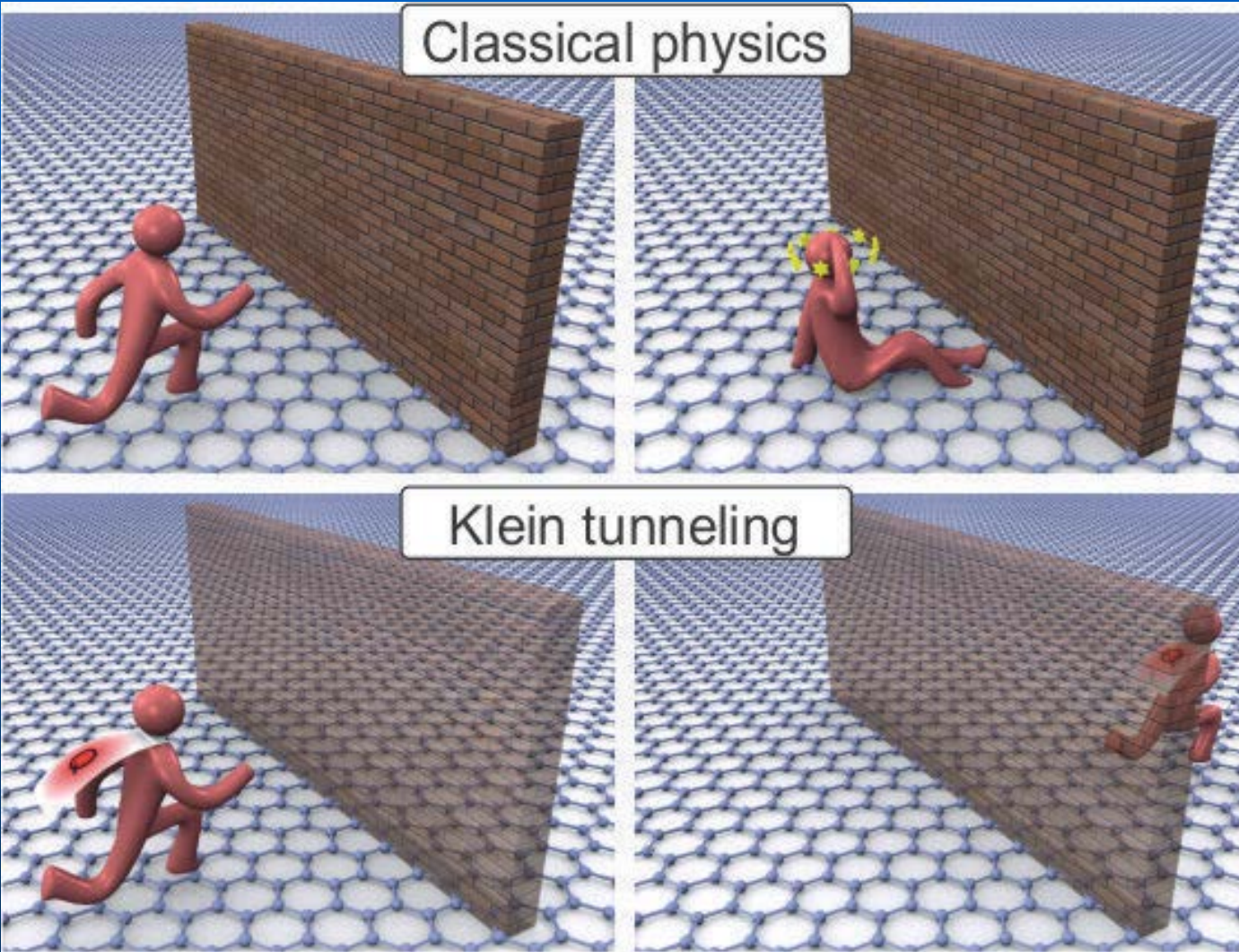
$$\beta = 2e^2/hG_0$$

$$\beta \ll \pi^2$$

Chiral tunneling and Klein paradox

MIK, Novoselov, Geim, Nat. Phys. 2, 620 (2006)

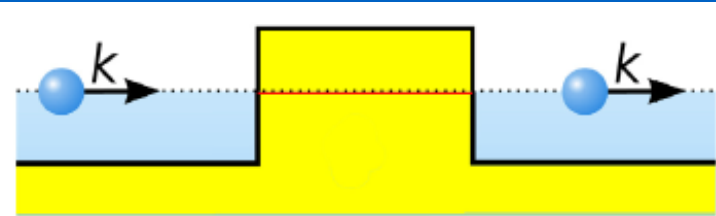
Electronics: heterostructures (p - n - p junctions etc.)



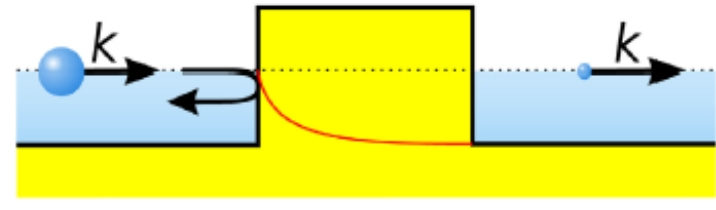
(C) Florian Sterl

Klein paradox II

Ultrarelativistic



Nonrelativistic



Tunnel effect: momentum and coordinate are complementary variables, kinetic and potential energy are not measurable simultaneously

Relativistic case: even the *coordinate itself* is not measurable, particle-antiparticle pair creation

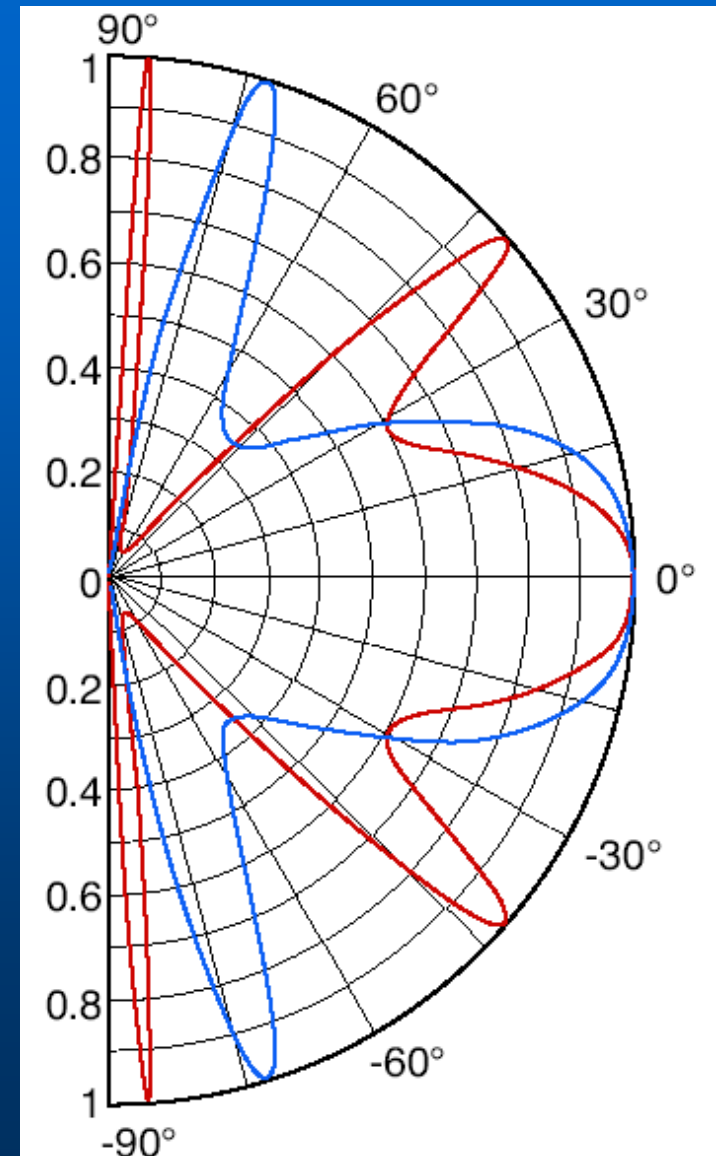
Klein paradox III

Transmission probability

Barrier width 100 nm

Electron concentration
outside barrier $0.5 \times 10^{12} \text{ cm}^{-2}$

Hole concentration
inside barrier $1 \times 10^{12} \text{ cm}^{-2}$ (red)
and $3 \times 10^{12} \text{ cm}^{-2}$ (blue)



Klein tunneling: Experimental confirmation

PRL **102**, 026807 (2009)

PHYSICAL REVIEW LETTERS

week ending
16 JANUARY 2009

Evidence for Klein Tunneling in Graphene *p-n* Junctions

N. Stander, B. Huard, and D. Goldhaber-Gordon*

Department of Physics, Stanford University, Stanford, California 94305, USA

(Received 13 June 2008; published 16 January 2009)

Transport through potential barriers in graphene is investigated using a set of metallic gates capacitively coupled to graphene to modulate the potential landscape. When a gate-induced potential step is steep enough, disorder becomes less important and the resistance across the step is in quantitative agreement with predictions of Klein tunneling of Dirac fermions up to a small correction. We also perform magnetoresistance measurements at low magnetic fields and compare them to recent predictions.

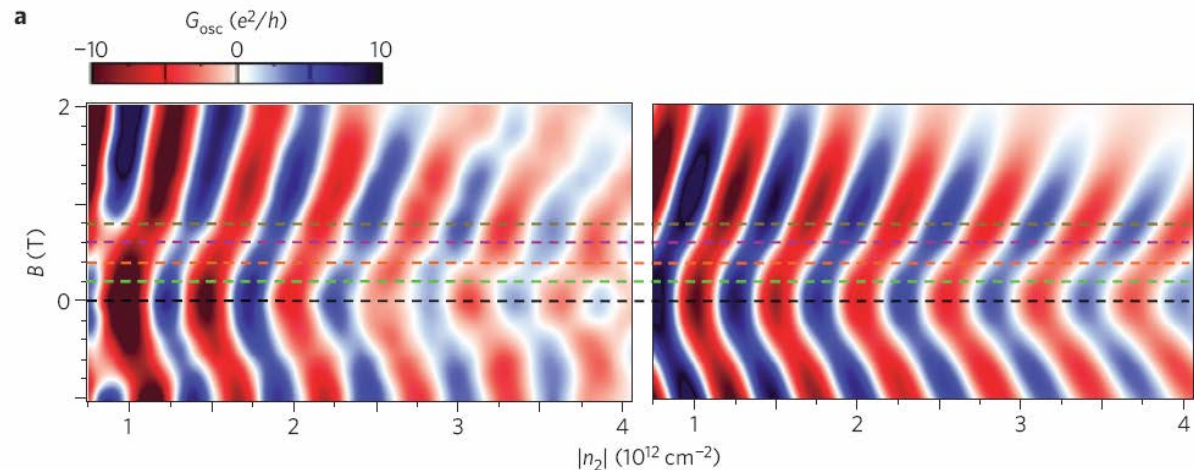
nature
physics

LETTERS

PUBLISHED ONLINE: 1 FEBRUARY 2009 | DOI: 10.1038/NPHYS1198

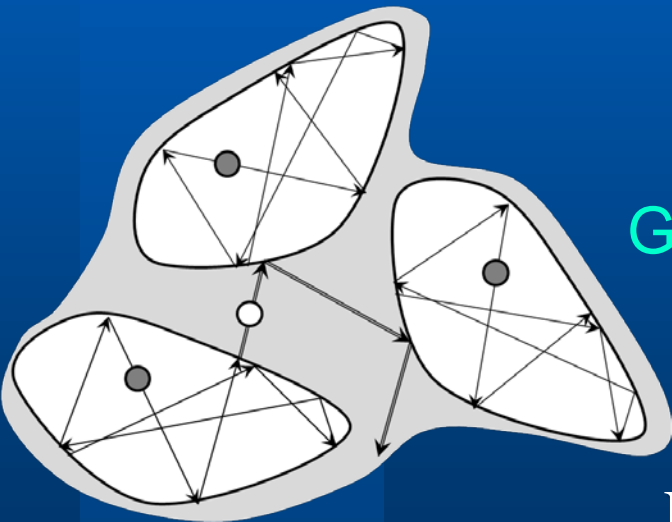
Quantum interference and Klein tunnelling in graphene heterojunctions

Andrea F. Young and Philip Kim*

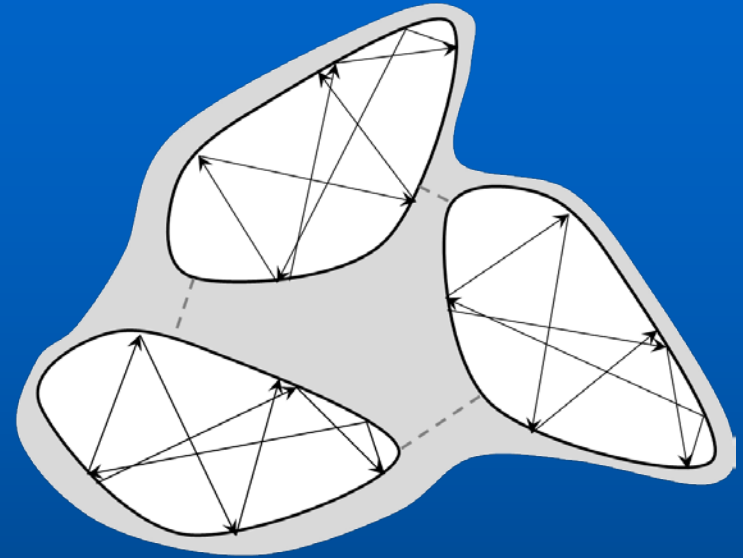


Klein tunneling prevents localization

Back scattering is
forbidden for chiral
fermions! Magic angle = 0
Nonuniversal magic angle
for bilayer exists!



Graphene



Conventional semiconductors

Electrons cannot be locked by random potential
relief neither for single-layer nor for bilayer
graphene – absence of localization and minimal
conductivity?!

Quantum-Limited Resistivity

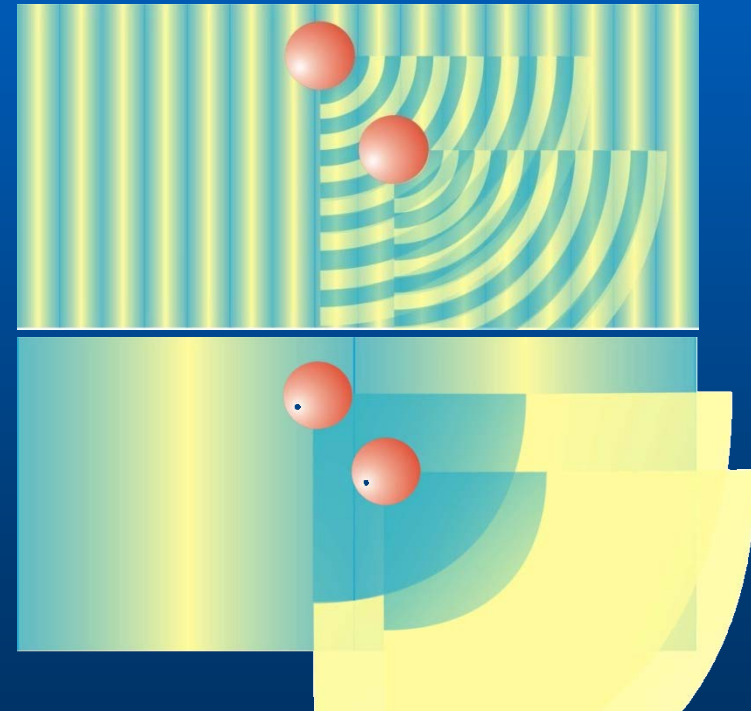
$$\sigma = ne\mu = \frac{e^2}{h} k_F l$$

Mott argument:

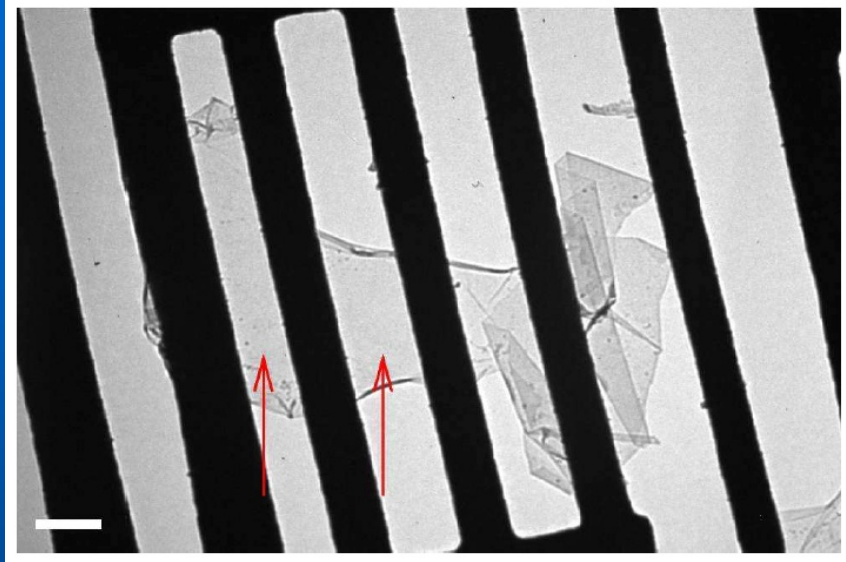
$$l \geq \lambda_F$$

$$\sigma \geq \frac{e^2}{h}$$

(in the absence of localization)



Inhomogeneities are unavoidable



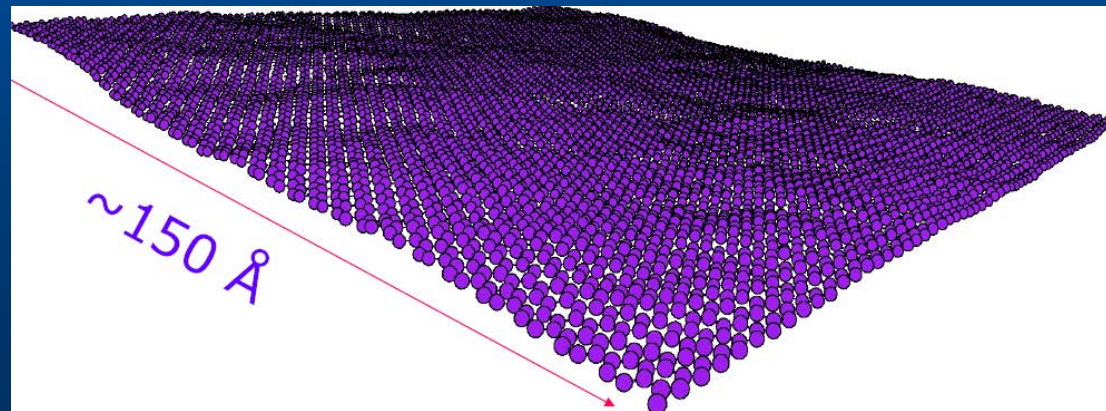
Freely suspended graphene membrane is corrugated

Meyer et al, *Nature* 446, 60 (2007)

2D crystals in 3D space cannot be flat, due to bending instability

Atomistic simulations of intrinsic ripples

Fasolino, Los & MUK,
Nature Mater. 6, 858 (2007)



Ripples and puddles

Gibertini, Tomadin, Polini, Fasolino & MIK, PR B 81, 125437 (2010)

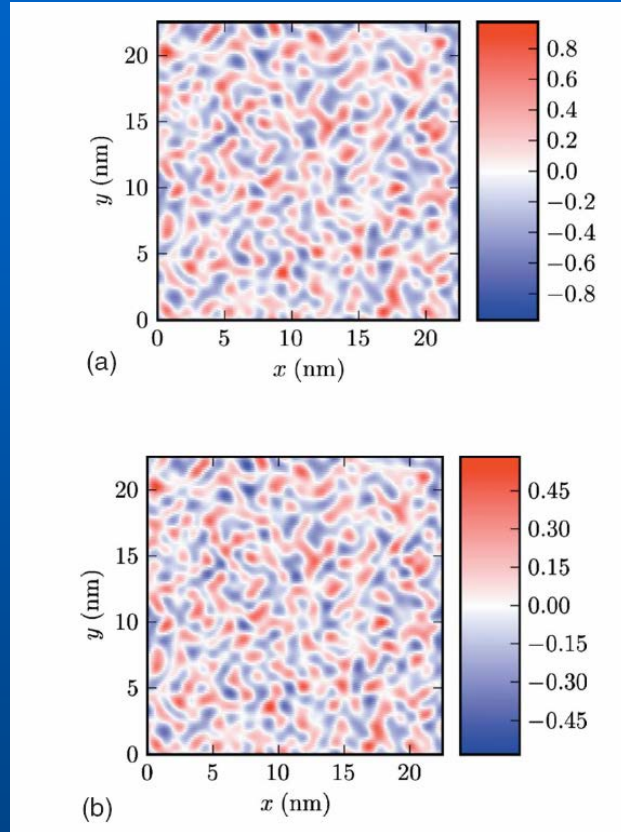


FIG. 4. (Color online) Top panel: fully self-consistent electronic density profile $\delta n(r)$ (in units of 10^{12} cm^{-2}) in a corrugated graphene sheet. The data reported in this figure have been obtained by setting $g_1=3 \text{ eV}$, $\alpha_{ee}=0.9$ (this value of α_{ee} is the commonly used value for a graphene sheet on a SiO_2 substrate), and an average carrier density $\bar{n}_c \approx 0.8 \times 10^{12} \text{ cm}^{-2}$. Bottom panel: same as in the top panel but for $\alpha_{ee}=2.2$ (this value of α_{ee} corresponds to suspended graphene).

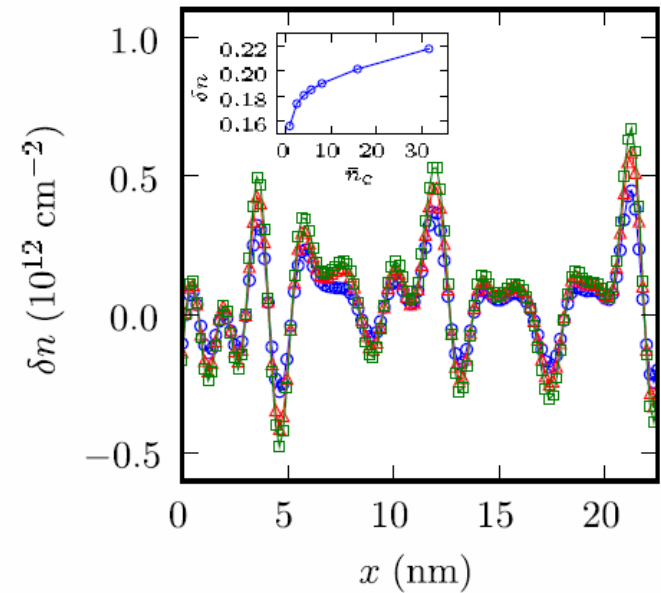


FIG. 9. (Color online) One-dimensional plots of the self-consistent density profiles (as functions of x in nm for $y=21.1 \text{ nm}$) for different values of doping: $\bar{n}_c \approx 0.8 \times 10^{12} \text{ cm}^{-2}$ (circles), $\bar{n}_c \approx 3.96 \times 10^{12} \text{ cm}^{-2}$ (triangles), and $\bar{n}_c \approx 3.17 \times 10^{13} \text{ cm}^{-2}$ (squares). The data reported in this figure have been obtained by setting $g_1=3 \text{ eV}$ and $\alpha_{ee}=2.2$. The inset shows $\delta n(r)$ (in units of 10^{12} cm^{-2}) at a given point r in space as a function of the average carrier density \bar{n}_c (in units of 10^{12} cm^{-2}).

Ripples and puddles II

Graphene on SiO₂

Gibertini, Tomadin, Guinea, MIK & Polini PR B 85, 201405 (2012)

Experimental STM data: V.Geringer et al (M.Morgenstern group)

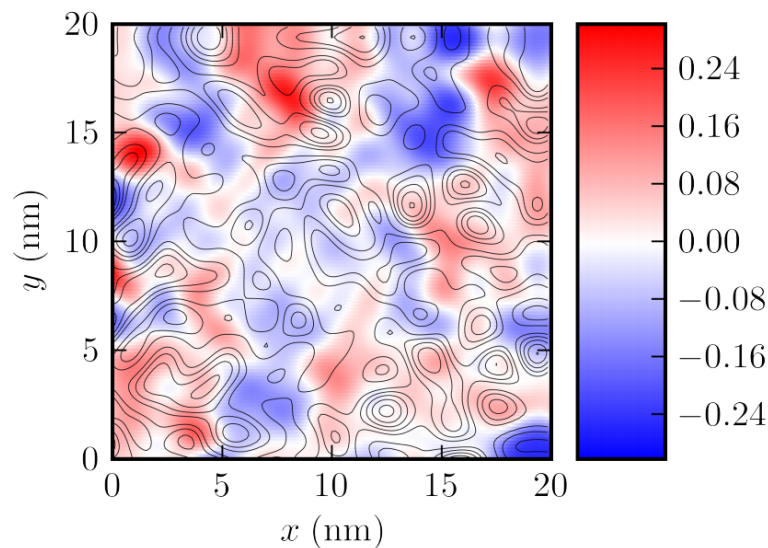
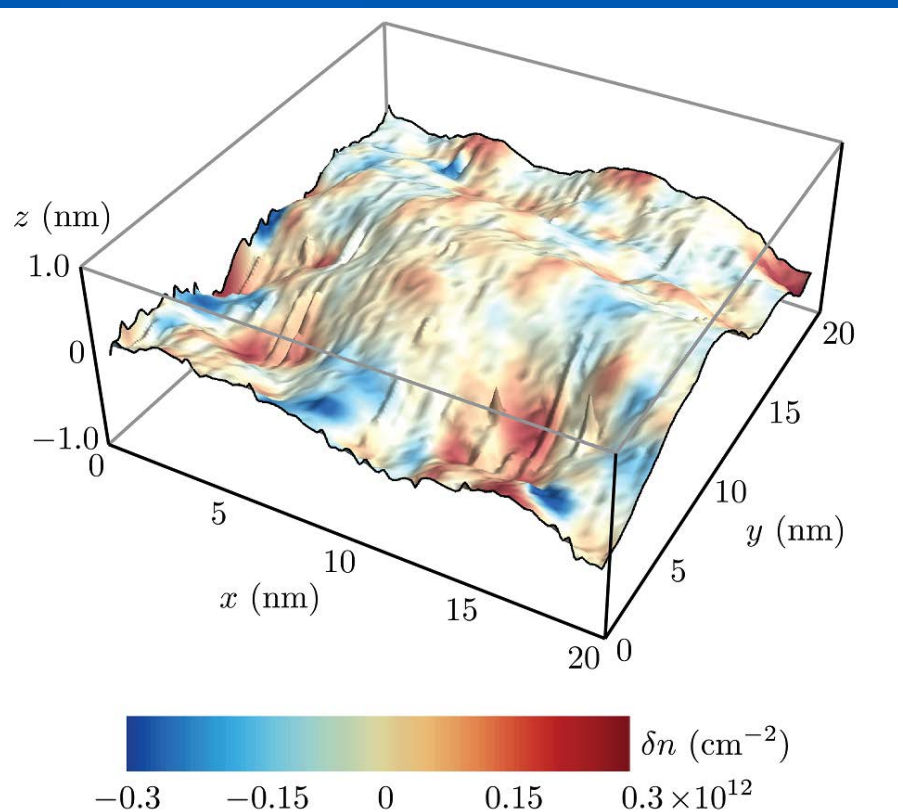


FIG. 3: (Color online) Fully self-consistent induced carrier-density profile $\delta n(\mathbf{r})$ (in units of 10^{12} cm^{-2}) in the corrugated graphene sheet shown in Fig. 1. The data reported in this figure have been obtained by setting $g_1 = 3 \text{ eV}$, $\alpha_{ee} = 0.9$, and an average carrier density $\bar{n}_c \approx 2.5 \times 10^{11} \text{ cm}^{-2}$. The thin solid lines are contour plots of the curvature $\nabla_r^2 h(\mathbf{r})$. Note that there is no simple correspondence between topographic out-of-plane corrugations and carrier-density inhomogeneity.

The role of Klein tunneling

Without Klein tunneling graphene near the neutrality point will be insulator and, anyway, will have a high enough mobility

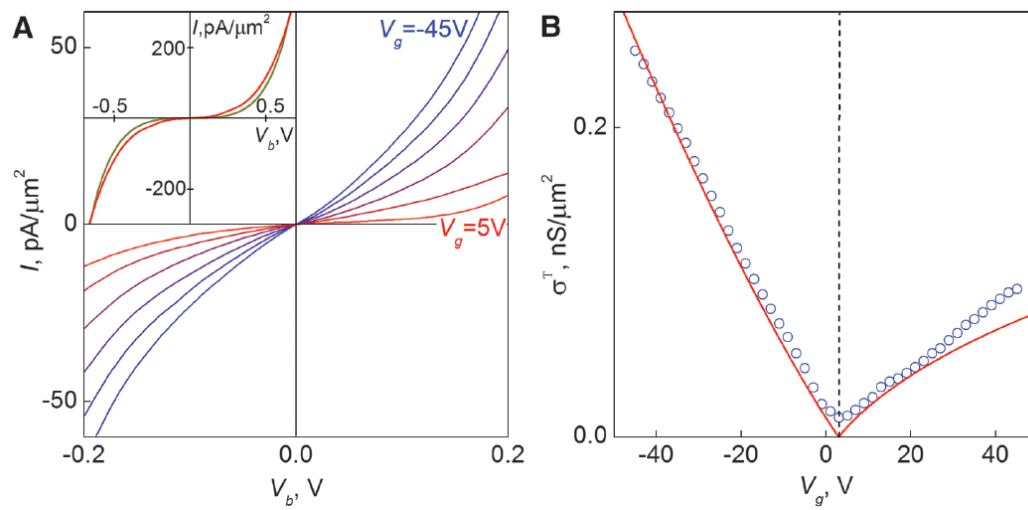
At the same time: a problem with transistors, one needs to use a complicated and indirect ways

Crucial phenomenon for physics and electronic applications of graphene

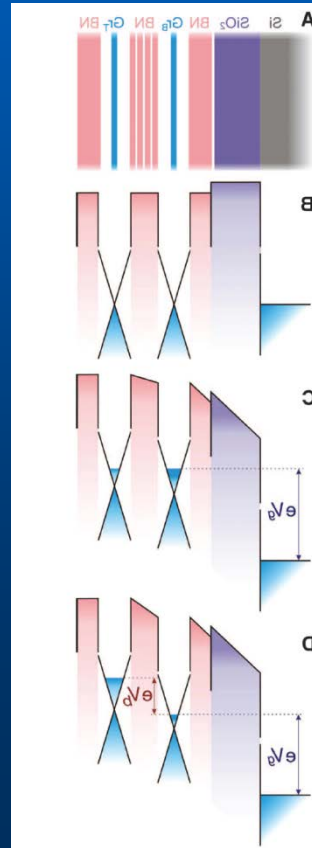
Field-Effect Transistor Based on Vertical Graphene Heterostructures

L. Britnell, *et al.*

Science **335**, 947 (2012);



Tunneling transistor with vertical geometry



Semiclassical theory

Tudorovkiy, Reijnders, MIK, Phys. Scr. T 146, 014010 (2012);
Reijnders, Tudorovskiy, MIK, Ann. Phys. (NY) 333, 155 (2013)

One-dimensional potential

$$\left[v \begin{pmatrix} 0 & \hat{p}_x - ip_y \\ \hat{p}_x + ip_y & 0 \end{pmatrix} + u(x/l) - E \right] \Psi = 0$$

$$\tilde{x} = x/l, \tilde{p}_x = -i\hbar d/d\tilde{x}, \tilde{p}_y = p_y/p_0, \hbar = \hbar/p_0 l, \tilde{u} = u/vp_0$$

$$\tilde{E} = E/vp_0$$

Skipping tildas: the Hamiltonian

$$\hat{H} = \begin{pmatrix} 0 & \hat{p}_x - ip_y \\ \hat{p}_x + ip_y & 0 \end{pmatrix} + u(x)$$

Semiclassical theory II

Reduction to exact Schrödinger equations for complex potential

$$(\hat{p}_x^2 + p_y^2 - v(x)^2 - i\hbar\sigma_x v'(x))\Psi = 0$$

$$v(x) = u(x) - E$$

$$\Psi = \begin{pmatrix} 1 \\ 1 \end{pmatrix} \eta_1 + \begin{pmatrix} 1 \\ -1 \end{pmatrix} \eta_2$$

$$\left(\hbar^2 \frac{d^2}{dx^2} + v(x)^2 - p_y^2 \pm i\hbar v'(x) \right) \eta_{1,2} = 0$$

Schrödinger equation with complex potential

Semiclasical theory III

Classical mechanics:

$$E = \pm |p| + u(x)$$

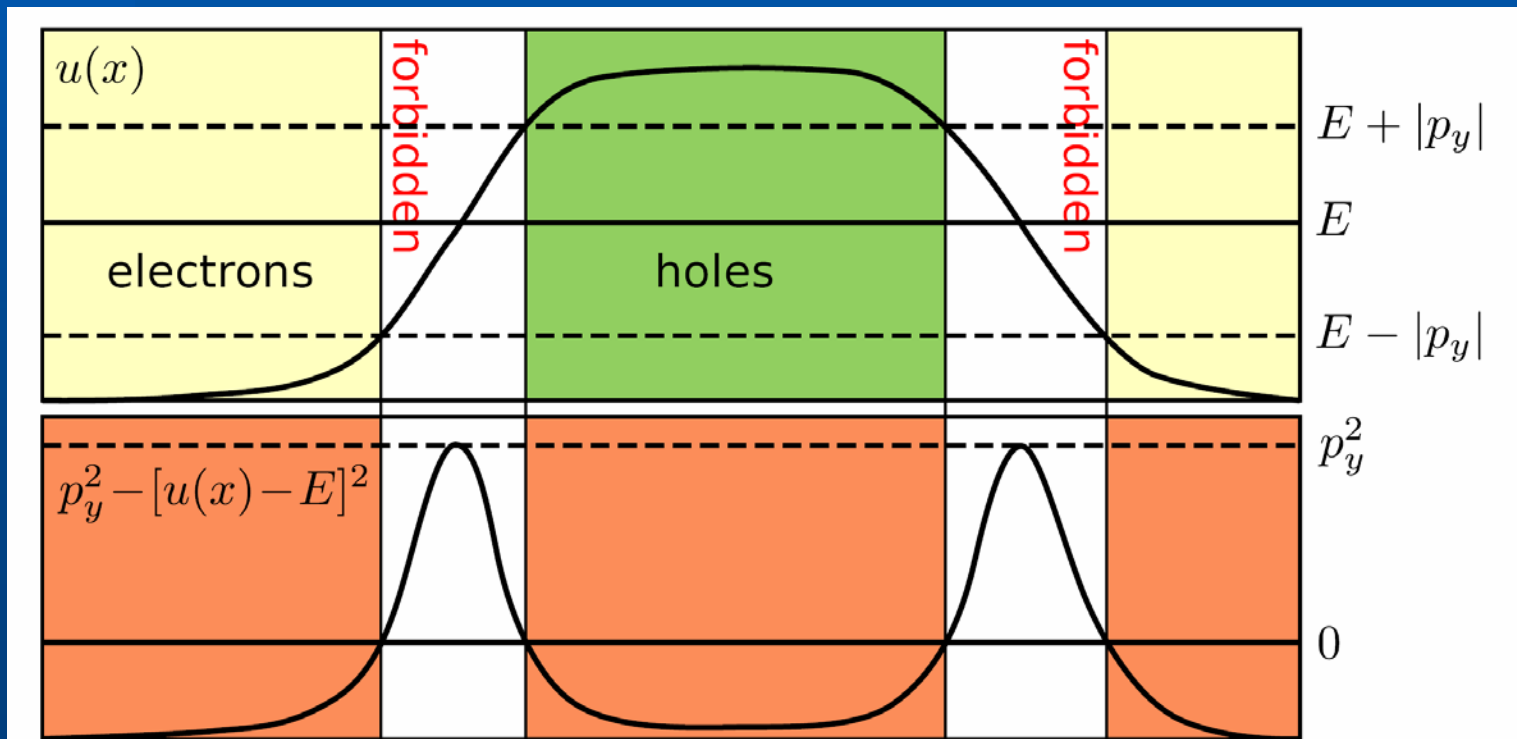
Effective Hamiltonian

$$\mathcal{L}(p_x, x) = p_x^2 - v^2(x) = -p_y^2$$

$$v(x) = u(x) - E$$

The case of Klein tunneling

$$E < U_{\max}, |p_y| < U_{\max} - E$$



p-n-p junction

Exact requirement: 100% transmission for normally incident wave
One needs to use comparison equation, exact solution for parabolic potential

Transmission probability

$$t_{npn} = \frac{e^{-K_{np}/h} e^{-K_{pn}/h} e^{-iL/h}}{1 - \sqrt{1 - e^{-K_{np}/h}} \sqrt{1 - e^{-K_{pn}/h}} e^{-2iL/h + i\pi - i\theta_{np} - i\theta_{pn}}}$$

$$K_{np} = \int_{x_1}^{x_2} dx \sqrt{p_y^2 - v^2(x)}$$

$X_{1,2}$ are turning points

$$v^2(x_0) - p_y^2 = 0$$

$$L = \int_{x_2}^{x_3} dx' \sqrt{v^2(x') - p_y^2}$$

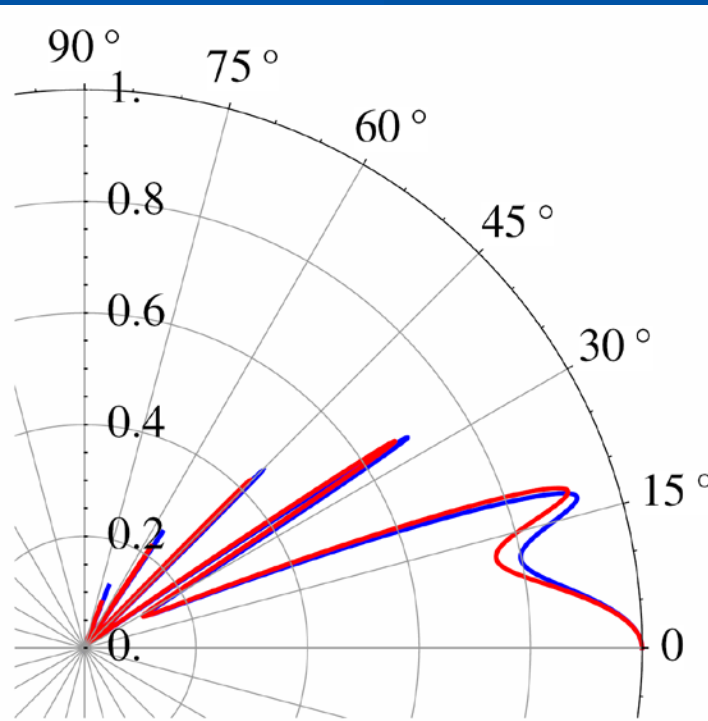
$$\theta = \text{Arg} \left[\Gamma \left(1 + i \frac{K}{\pi h} \right) \right] - \frac{\pi}{4} + \frac{K}{\pi h} - \frac{K}{\pi h} \ln \left(\frac{K}{\pi h} \right)$$

Fabri-Perot resonances

Magic angles with 100% transmission survives only for symmetric barriers (except normal incidence)

$$|t_{\text{res}}| = \frac{1}{\cosh(K_{np}/h - K_{pn}/h)}$$

$$K_{np}/h \gg 1, K_{pn} \gg 1$$



$$u(x/l_1) = \frac{u_{\text{max}}}{2} \left[1 + \tanh \left(10 \frac{x}{l_1} - 5 \right) \right]$$

The angular dependence of the transmission coefficient for a particle of energy 80 meV incident on an n-p-n junction of height 200 meV. The barrier width $l_2 = 250$ nm and the n-p and p-n regions have characteristic lengths $l_1 = 150$ nm and $l_3 = 50$ nm, respectively. The blue line shows the numerical results for 99 steps, while the red line shows the uniform approximation (5.77).

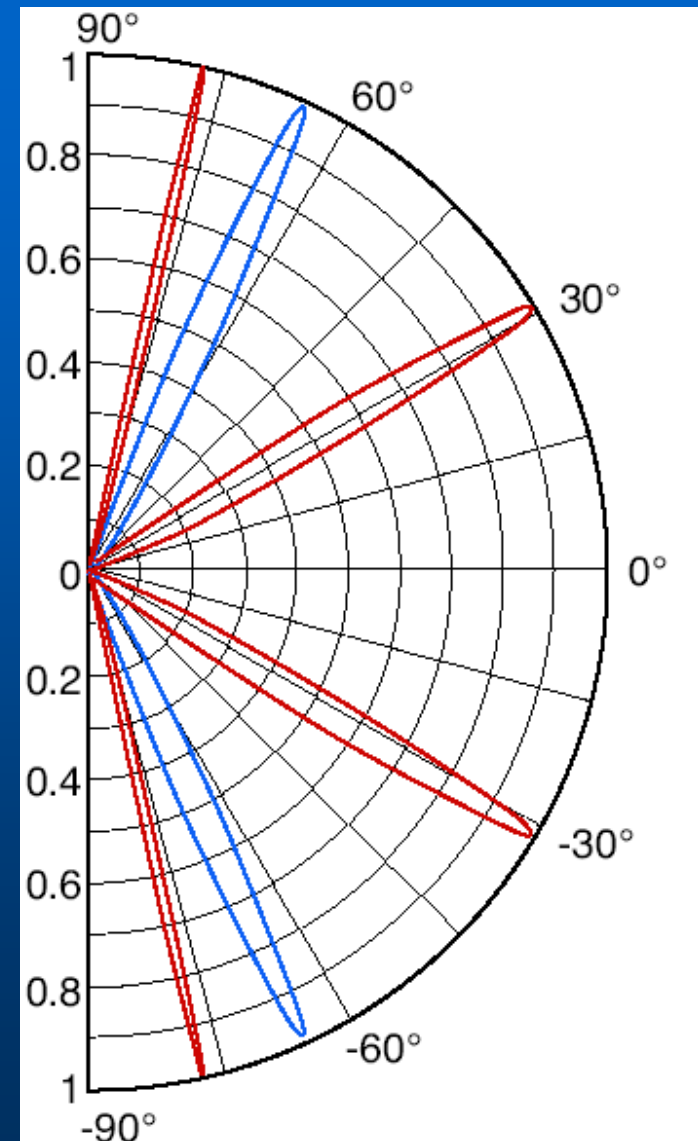
Very nice agreement with numerics

Chiral tunneling - bilayer

Problem: graphene transistor
can hardly be locked!

Possible solution: use bilayer
graphene: chiral fermions with
parabolic spectrum – no analogue
in particle physics!

Transmission for bilayer;
parameters are the same as for
previous slide



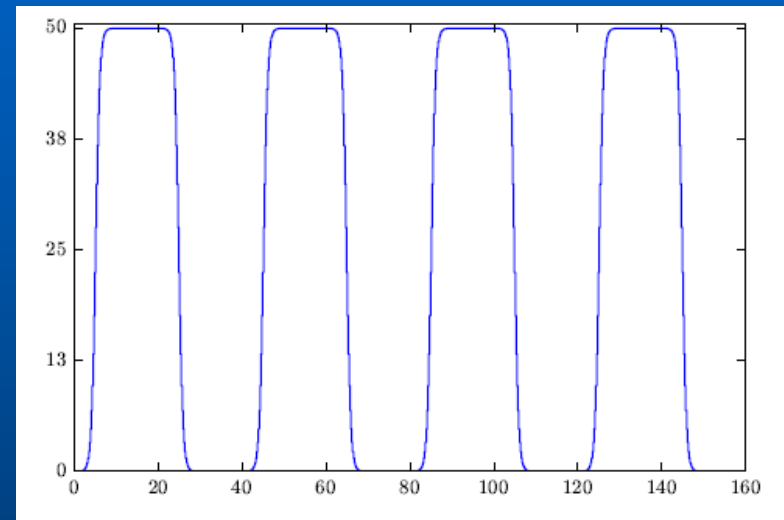
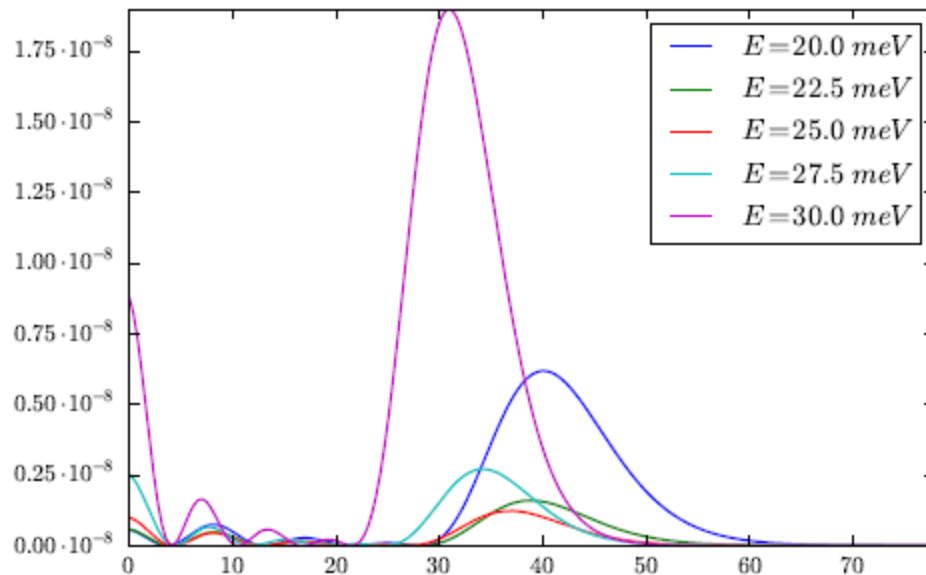
Chiral tunneling – bilayer II

Kleptsyn, Okunev, Schurov, Zubov & MIK, PRB **92**, 165407 (2015)

For symmetric potential $V(x)=V(-x)$: one real equation for magic angles but not necessarily real solutions

Magic angles are not protected

Example: fast-oscillating potential



Very small transmission probability

From analysis of ODE to graphene transistor?!

Relativistic collapse for supercritical charges

Coulomb potential

$$V_0(\mathbf{r}) = \frac{Ze^2}{\epsilon r}$$

following Shytov, MIK & Levitov, PRL 99, 236801;
246803 (2007)

Naive arguments: Radius of atom R ,
momentum \hbar/R . Nonrelativistic case:

$$E(R) \sim \hbar^2 / mR^2 - Ze^2/R$$

Minimum gives a size of atom.

Relativistic case: $E(R) \sim \hbar c^*/R - Ze^2/R$

Either no bound state or fall on the center.

Vacuum reconstruction at $Z > 170$

Supercritical charges II

Superheavy
nuclei

Graphene:
 $v \approx c/300$,
 $\alpha_{eff} \approx 1$

I. Pomeranchuk and Y. Smorodinsky, J. Phys. USSR **9**, 97 (1945)

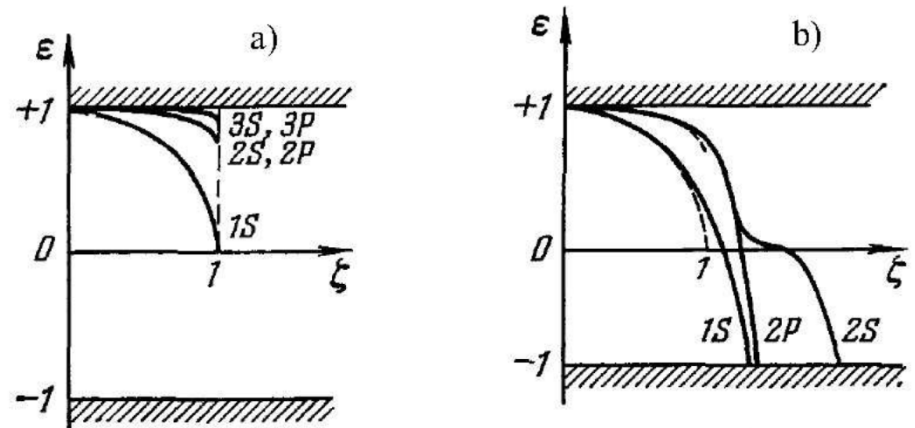
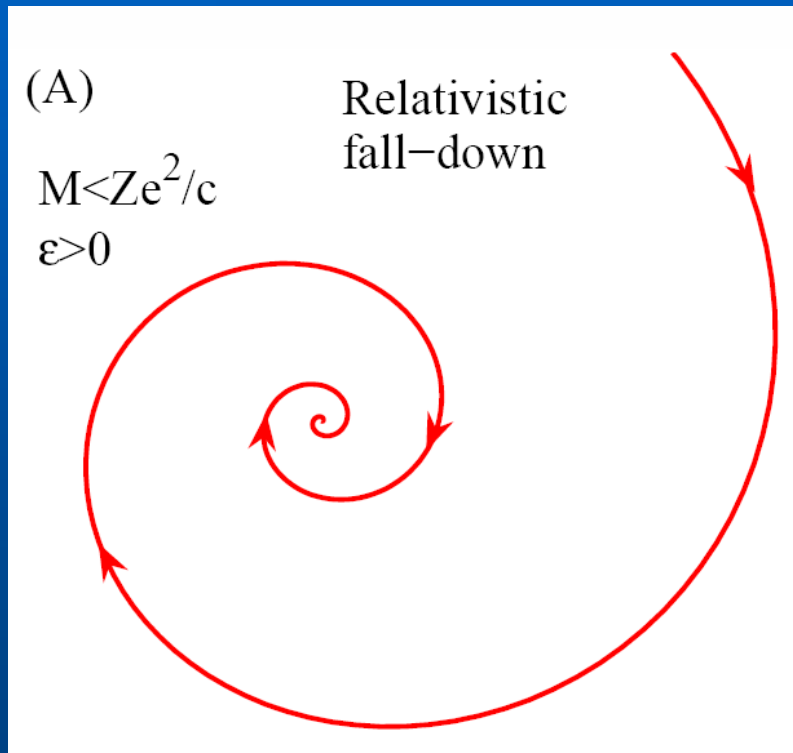


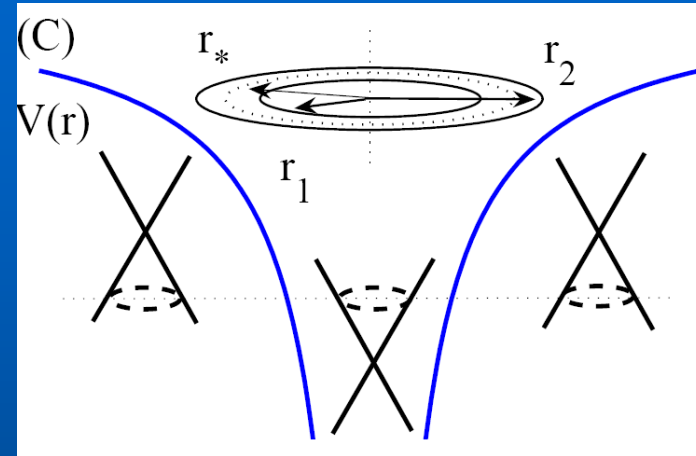
FIG. 1: a) Energy levels of superheavy atoms obtained from Dirac equation for Coulomb potential $-Ze^2/r$, plotted as a function of $\zeta = Z\alpha$, where Z is nuclear charge, and $\alpha = e^2/\hbar c$ is the fine structure constant. Energy is in the units of mc^2 . (b) Energy levels for Coulomb potential regularized on the nuclear radius. As Z increases, the discrete levels approach the continuum of negative-energy states and dive into it one by one at supercritical $Z > 170$ (from Ref.[23]).

Supercritical charges III

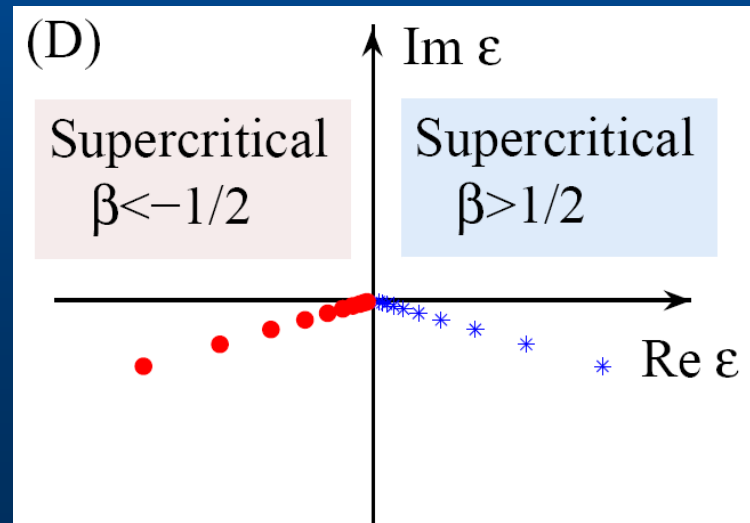
$$\beta = Ze^2/\hbar v_F \epsilon > 1/2$$



Quasi-local states

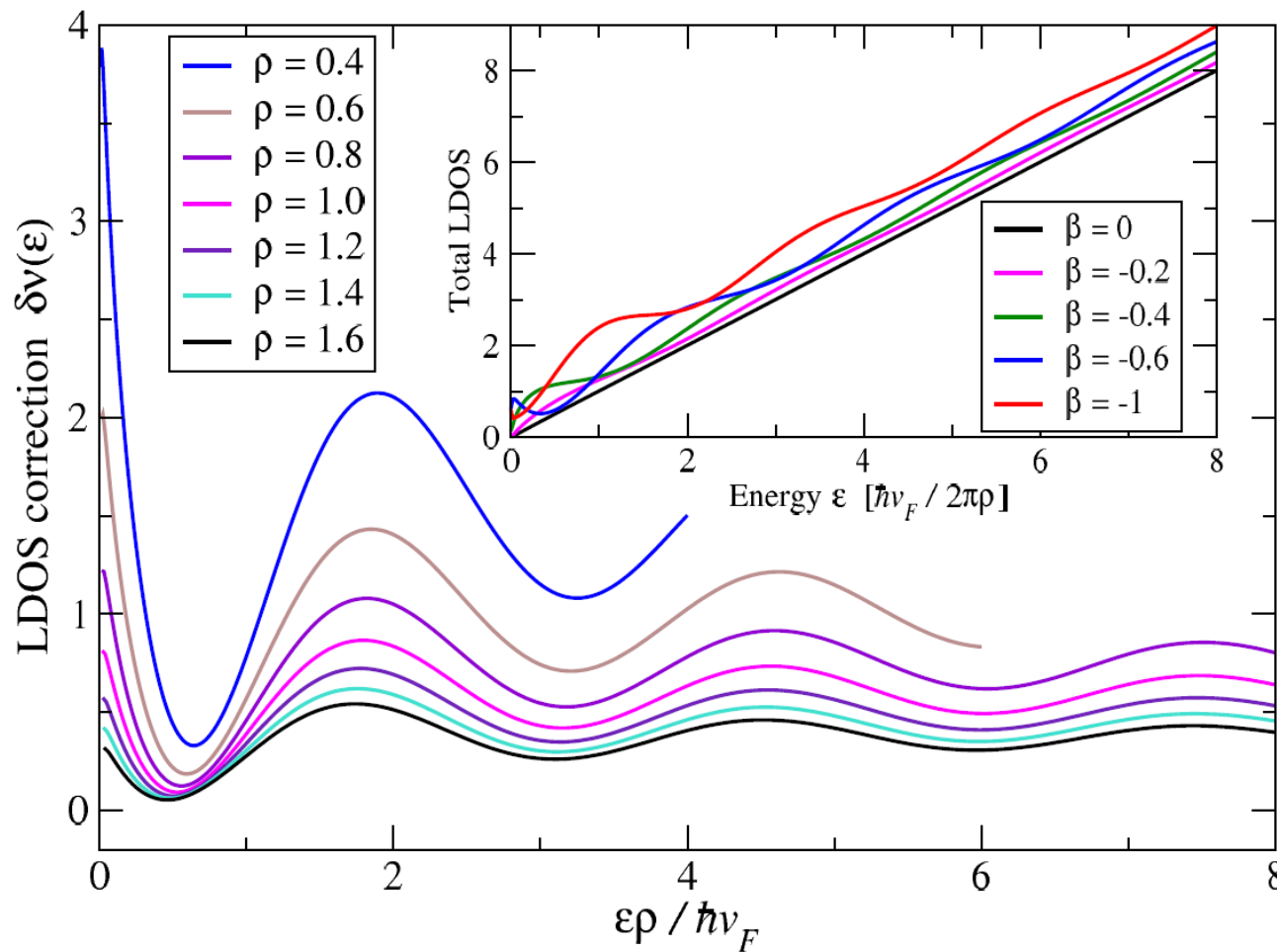


Klein tunneling



Supercritical charges IV

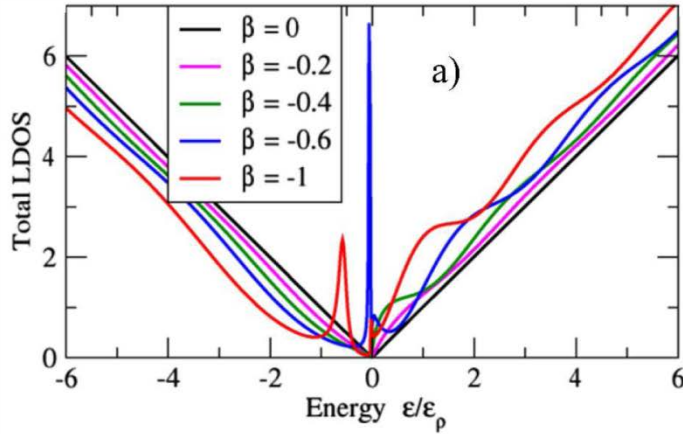
Interference of scattered wave and wave described electron fall to the centre leads to oscillations of electron density



$\beta = 0.6$

Inset:
oscillations
for different
charges

Supercritical charge V



A. V. Shytov, M. I. Katsnelson, and L. S. Levitov, Phys. Rev. Lett. **99**, 236801 (2007), arXiv:0705.4663

A. V. Shytov, M. I. Katsnelson, and L. S. Levitov, Phys. Rev. Lett. **99**, 246802 (2007), arxiv.org:0708.0837

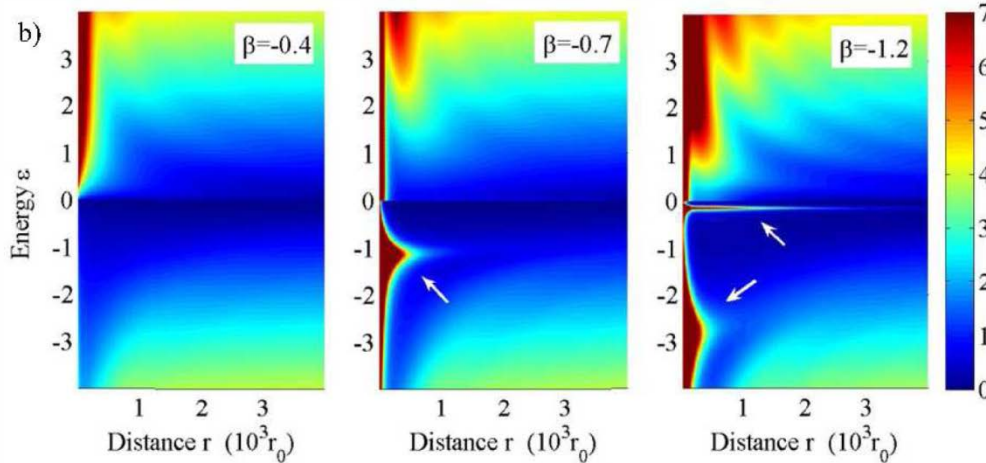


FIG. 3: (a) Local density of states (12) calculated at a fixed distance $\rho = 10^3 r_0$ from the charged impurity, where r_0 is a short-distance parameter of the order of carbon lattice spacing (from Ref.[10]). Peaks in the LDOS, which appear at supercritical β and move to more negative energies at increasing $|\beta|$, correspond to the resonant states. (b) Spatial map of the density of states, shown for several values of β , with resonances marked by white arrows (from Ref.[11]). Note that the spatial width of the resonances decreases as they move to lower energies, $\Delta\rho \propto 1/|\varepsilon|$, while the linewidth increases, $\gamma \propto |\varepsilon|$. The oscillatory structure at positive energies represents standing waves with maxima at $k\rho \approx (n + \frac{1}{2})\pi$, similar to those studied in carbon nanotubes [26]. Energy is given in the units of $\varepsilon_0 = 10^{-3}\hbar v/r_0 \approx 30$ mV for $r_0 = 0.2$ nm.

Vacuum polarization effect and screening

Dimensional analysis: induced charge density in undoped graphene

$$n(r) = A\delta(r) + B/r^2$$

If B is not zero: logarithmically divergent induces charge and “nullification” of Coulomb potential – predicted by Thomas –Fermi theory

MIK, PR B 74, 201401 (2006)

Linear screening theory: constant dielectric function, screening charge focused at the coordinate origin (only first term)

Screening II

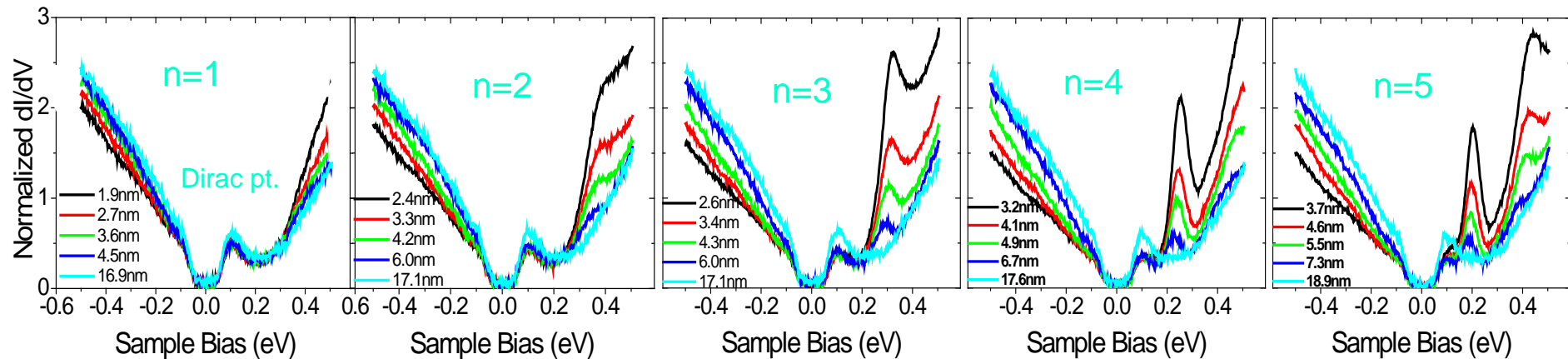
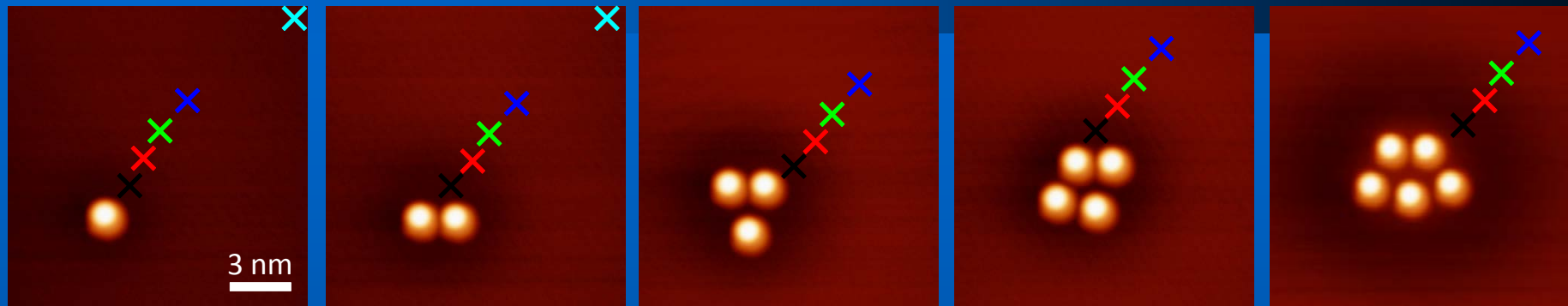
$$n_{\text{pol}}(\rho) = -\frac{N \operatorname{sign} \beta}{2\pi^2 \rho^2} \sum_{|m + \frac{1}{2}| < |\beta|} \sqrt{\beta^2 - \left(m + \frac{1}{2}\right)^2}$$

$N = 4$ (two valleys, two spins)

Large β : replacing the sum by an integral
recover the Thomas-Fermi result

RG analysis: supercritical charge is screened to
 $\beta = 1/2$ with a finite screening radius (similar
to black hole horizon)

Exper.: Tuning Z by Building Artificial Nuclei from Ca Dimers



Y. Wang et al, Science 340, 734 (2013)

Pseudomagnetic fields

Nearest-neighbour approximation: changes of hopping integrals

$$\gamma = \gamma_0 + \left(\frac{\partial \gamma}{\partial \bar{u}_{ij}} \right)_0 \bar{u}_{ij}$$

$$H = v_F \sigma \left(-i\hbar \nabla - \frac{e}{c} \mathcal{A} \right)$$

“Vector potentials”

$$\begin{aligned} \mathcal{A}_x &= \frac{c}{2ev_F} (\gamma_2 + \gamma_3 - 2\gamma_1), \\ \mathcal{A}_y &= \frac{\sqrt{3}c}{2ev_F} (\gamma_3 - \gamma_2), \end{aligned}$$

K and K' points are shifted in opposite directions;
Umklapp processes restore time-reversal symmetry

Review: M. Vozmediano, MLK & F. Guinea, Phys. Rep. 496, 109 (2010)

Pseudomagnetic fields II

Within elasticity theory (continuum limit)

$$\mathbf{A} = \frac{\beta}{a} \begin{pmatrix} u_{xx} - u_{yy} \\ -2u_{xy} \end{pmatrix}$$

$$\beta = -\partial \ln t / \partial \ln a \approx 2$$

Pseudomagnetic
field

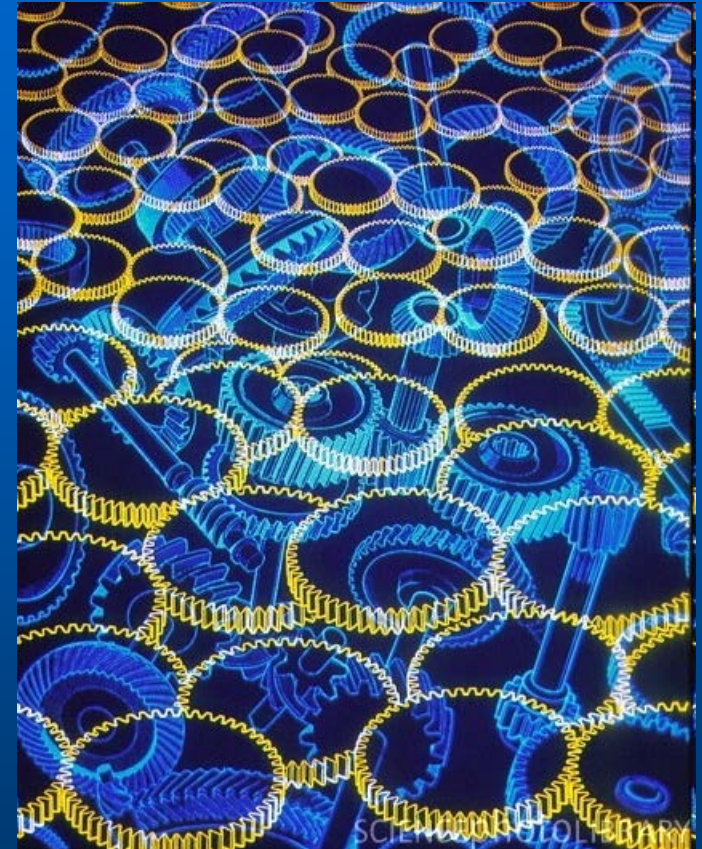
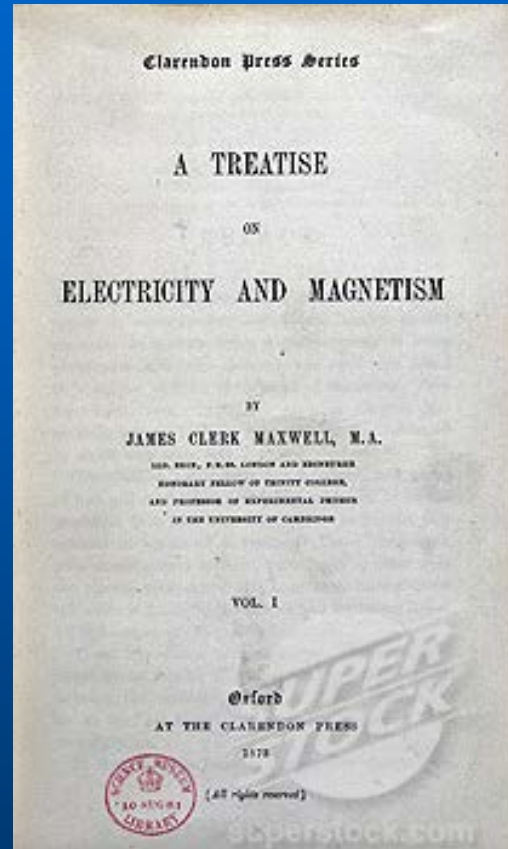
Shear deformations
create vector potential

$$B_s = \frac{\partial A_y}{\partial x} - \frac{\partial A_x}{\partial y} = \frac{1}{r} \frac{\partial A_r}{\partial \theta} - \frac{\partial A_\theta}{\partial r} - \frac{A_\theta}{r}$$

Dilatation creates scalar
(electrostatic) potential

$$V_1 = g_1(u_{xx} + u_{yy})$$

Gauge fields from mechanics: back to Maxwell



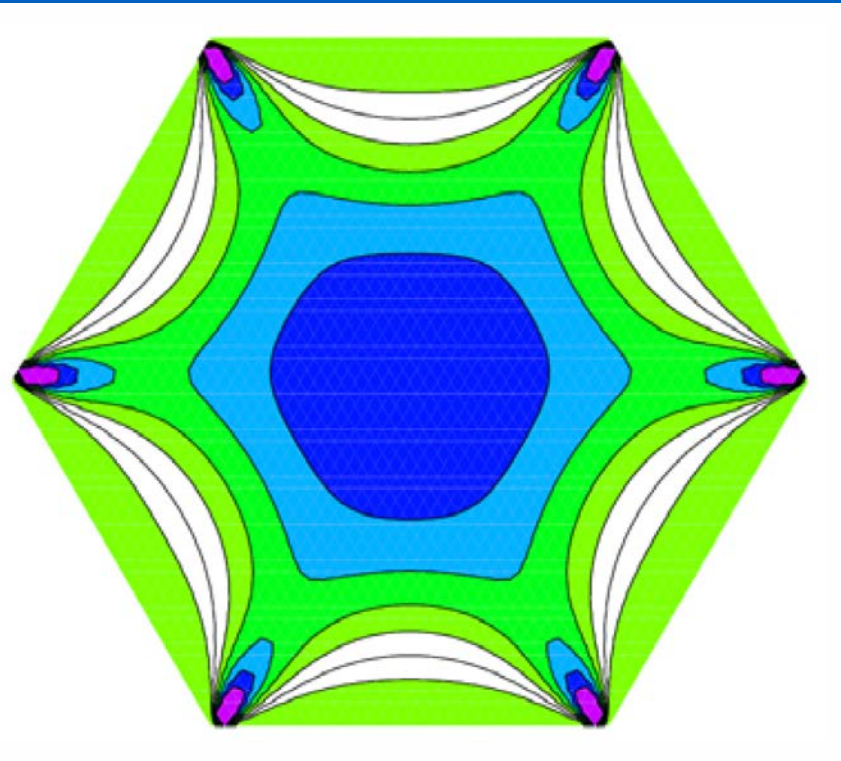
Electromagnetic fields as deformations
in ether; gears and wheels

Review: Vozmediano, MIK & Guinea, Phys. Rep. 496, 109 (2010)

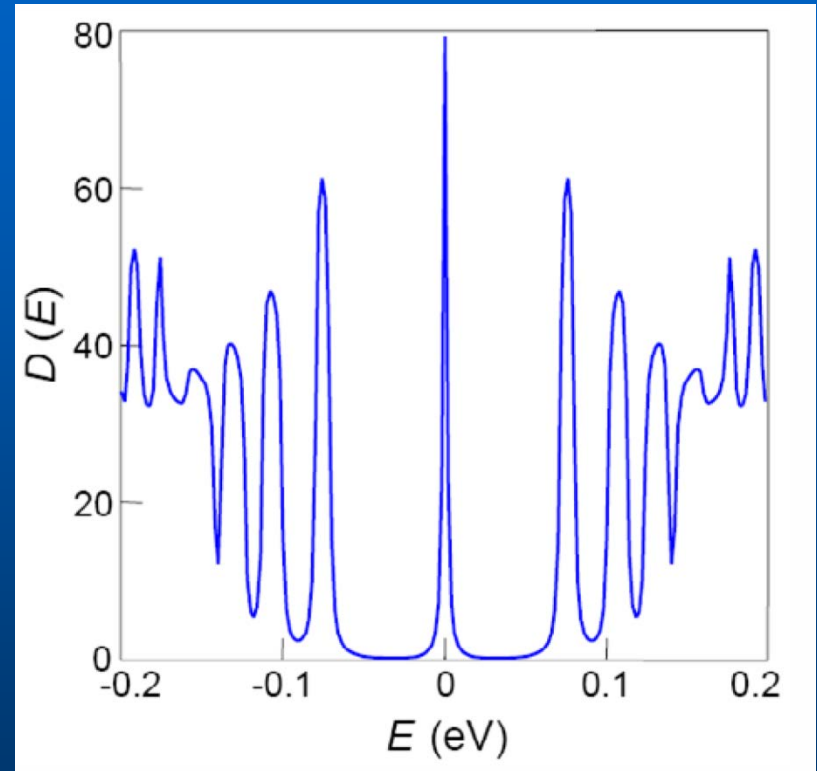
Zero-field QHE by strain engineering

F. Guinea, MIK & A. Geim, Nature Phys. 6, 30 (2010)

Can we create uniform (or almost uniform) pseudomagnetic field?



If you keep trigonal symmetry,
quasi-uniform pseudomagnetic field
can be easily created



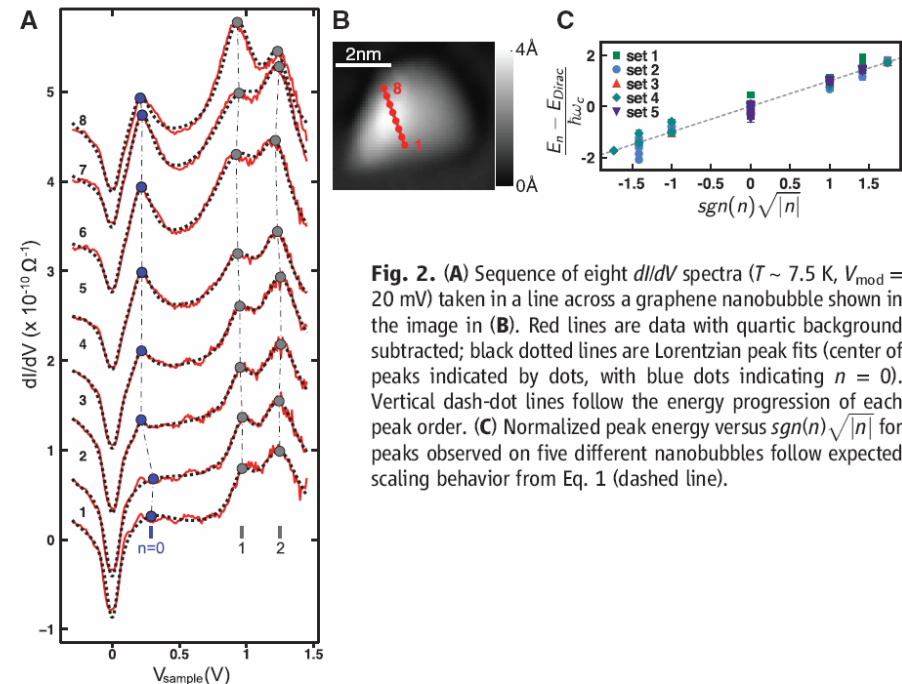
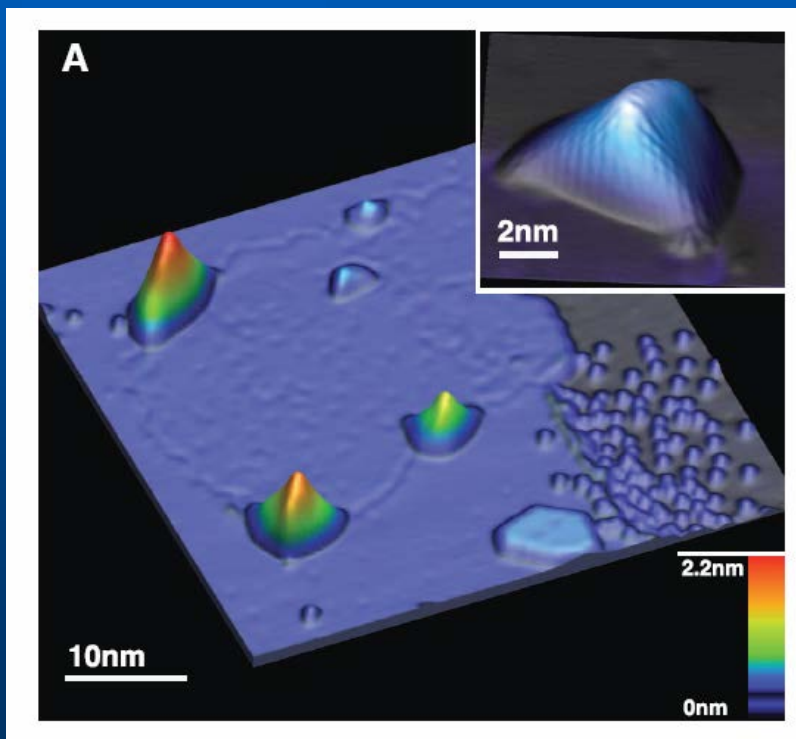
Normal stress applied to three edges
size $1.4 \mu\text{m}$, DOS in the center ($0.5 \mu\text{m}$)

Experimental confirmation

Strain-Induced Pseudo-Magnetic Fields Greater Than 300 Tesla in Graphene Nanobubbles

N. Levy,^{1,2*†} S. A. Burke,^{1*‡} K. L. Meaker,¹ M. Panlasigui,¹ A. Zettl,^{1,2} F. Guinea,³ A. H. Castro Neto,⁴ M. F. Crommie^{1,2§}

30 JULY 2010 VOL 329 SCIENCE



Graphene on Pt(111)

STM observation of pseudo-Landau levels

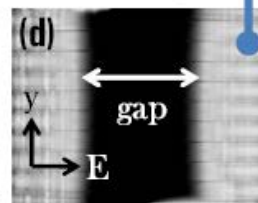
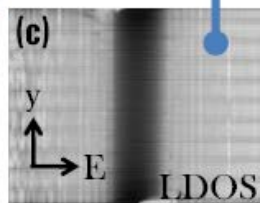
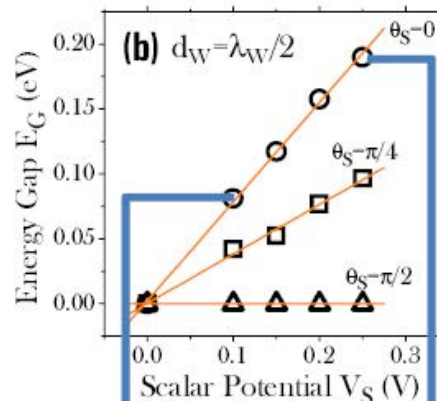
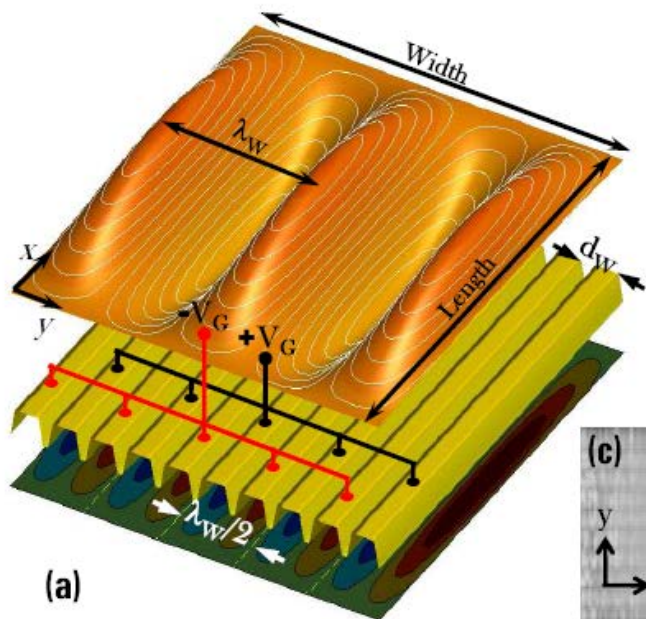
Combination of strain and electric field: Haldane insulator state

T. Low, F. Guinea & MIK, PRB 83, 195436 (2011)

Without inversion center
combination of vector and
scalar potential leads to gap
opening

$$\Delta = -\text{Tr} \left\{ \sigma_z \frac{2}{v_F} \int d^2 \vec{k} \frac{\text{Im}(V_{-\vec{k}})}{|\vec{k}|^2} [(\vec{k}\vec{\sigma}), (\vec{A}_{\vec{k}}\vec{\sigma})] \right\}$$

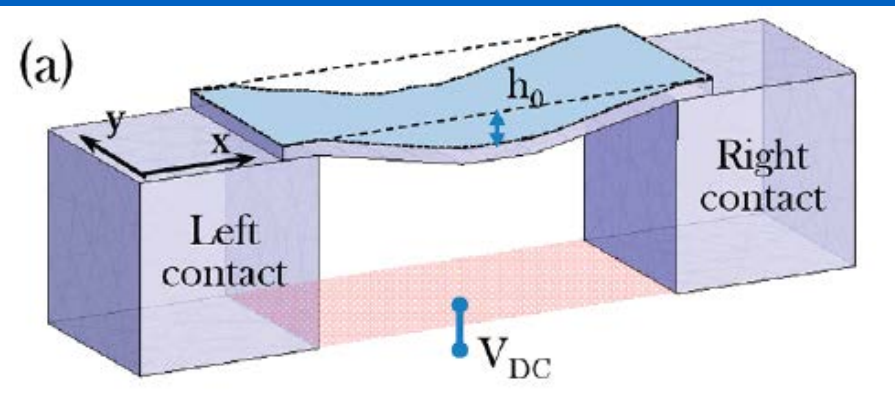
$$\propto \int d^2 \vec{k} \frac{\text{Im}(V_{-\vec{k}})}{|\vec{k}|^2} (k_x A_{\vec{k}}^y - k_y A_{\vec{k}}^x) \quad (1)$$



Wrinkles plus
modulated scalar
potential at different
angles to the wrinkling
direction

Quantum pumping

T. Low, Y. Jiang, MIK & F. Guinea Nano Lett. 12, 850 (2012)



Nanoelectromechanical resonator, periodic change of electric fields and pseudomagnetic fields (deformations) – a very efficient quantum pumping

Periodic electrostatic doping *plus* vertical deformation $a(t)$ created pseudomagnetic vector potential

$$V(t) = V_{\text{dc}} + V_{\text{ac}} \cos(\omega t)$$

$$\varepsilon_d = \hbar v_f (\pi C_T V_{\text{dc}} / e)^{1/2}$$

$$\mathcal{E}_{dg}(t) = \varepsilon_d \{1 + \delta\varepsilon_d \sin(\omega t)\}^{1/2}$$

$$\delta\varepsilon_d = V_{\text{ac}} / V_{\text{dc}}$$

$$u_{xx} = 8h_0^2 / 3L^2$$

$$\delta u_{xx} = a / h_0$$

$$\mathcal{U}_{xx}(t) = u_{xx} \{1 + \delta u_{xx} \sin(\omega t + \phi)\}^2 - \frac{\Delta L}{L}$$

Quantum pumping II

Scattering problem

$$\psi_j(x) = \begin{cases} \begin{pmatrix} 1 \\ \eta_l \end{pmatrix} e^{ik_{xl}x} + \mathcal{R}_v \begin{pmatrix} 1 \\ -\eta_l^\dagger \end{pmatrix} e^{-ik_{xl}x} \\ \alpha_l \begin{pmatrix} 1 \\ \eta_g \end{pmatrix} e^{ik_{xg}x} + \alpha_g \begin{pmatrix} 1 \\ -\eta_g^\dagger \end{pmatrix} e^{-ik_{xg}x} \\ \mathcal{T}_v \sqrt{\frac{k_{xl}k_{fr}}{k_{xr}k_{fl}}} \begin{pmatrix} 1 \\ \eta_r \end{pmatrix} e^{ik_{xr}x} \end{cases}$$

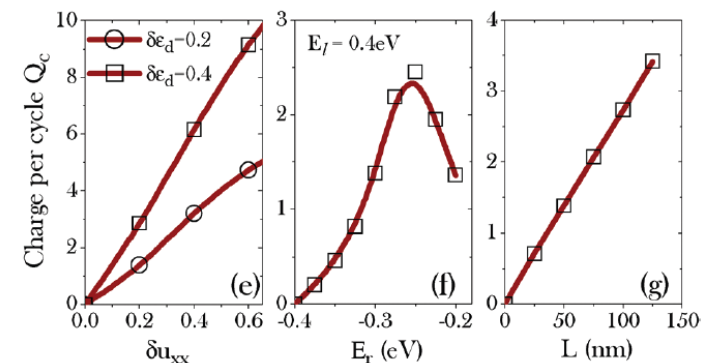
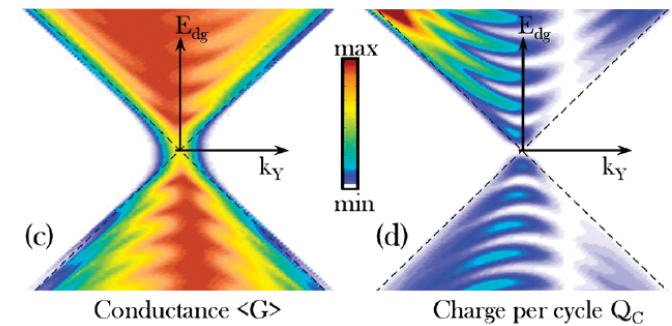
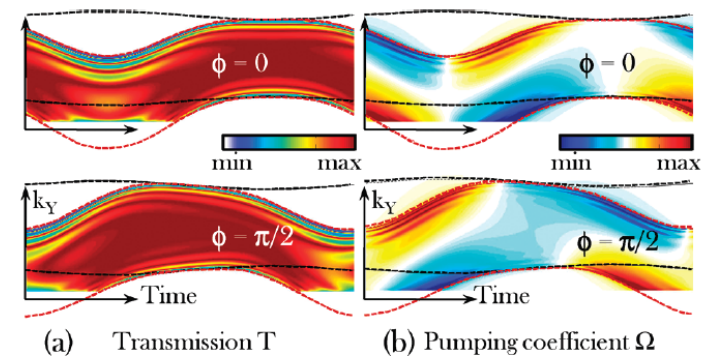
Pumping current

$$\mathcal{I}_v = i \frac{e\omega}{4\pi^2} \sum_{k_y} \int_0^{2\pi/\omega} dt \int_{-\infty}^{\infty} d\varepsilon \frac{\partial f_0(\varepsilon)}{\partial \varepsilon} \Omega_v(k_y, t)$$

$$\Omega_v = (\partial \mathcal{T}_v / \partial t) \mathcal{T}_v^\dagger + (\partial \mathcal{R}_v / \partial t) \mathcal{R}_v^\dagger$$

Asymmetric leads (different doping)

Results



Beyond the talk

Graphene on hBN: tunable incommensurate potential, very rich quantum and statistical mechanics

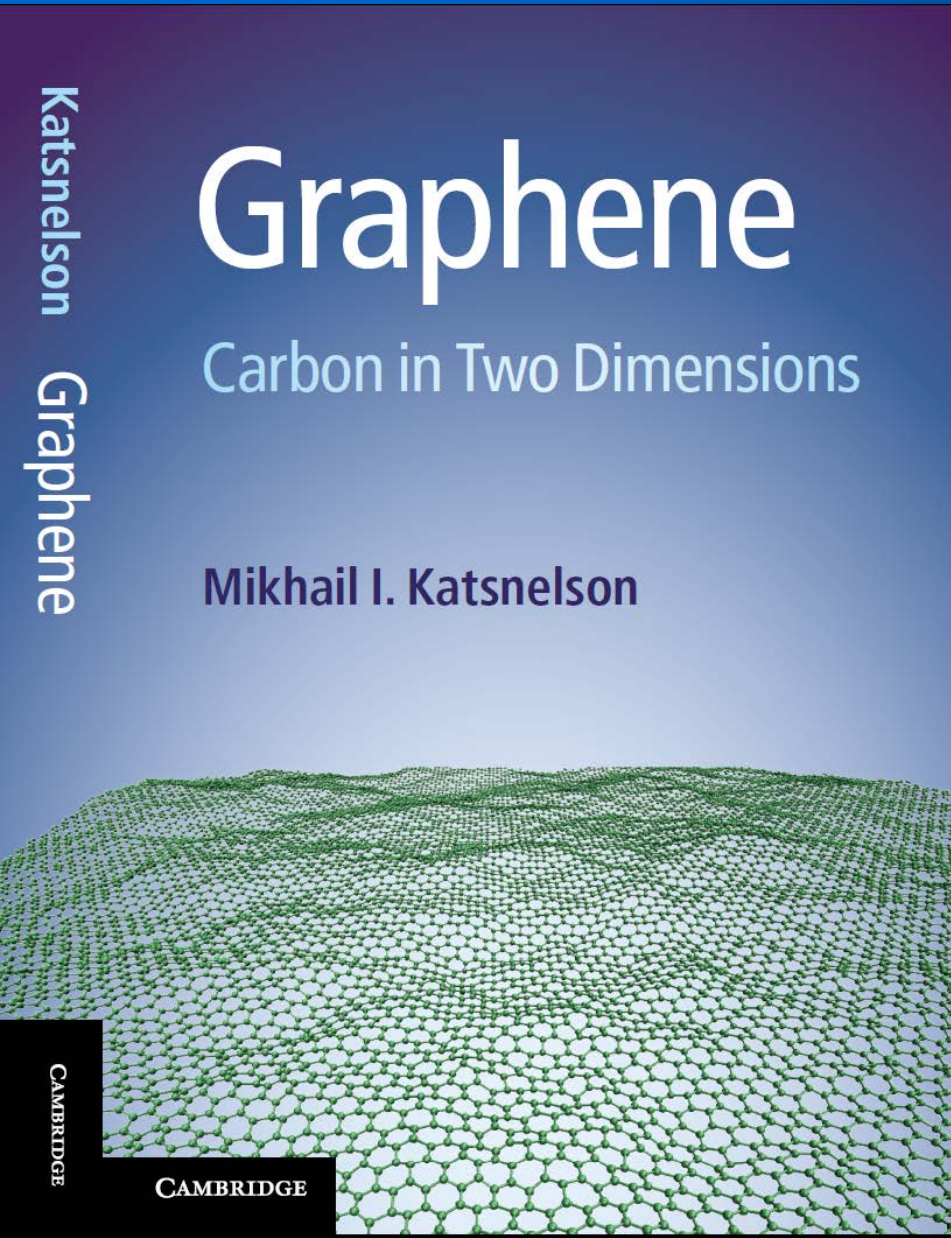
Graphene as a prototype crystalline membrane: Ripples and all that

Many-body effects – we are just in the beginning

Other 2D materials (especially, black P which can be made anisotropic Dirac material)

....

Further reading



Many thanks to all my collaborators from Nijmegen, Manchester, Madrid, Hamburg, Helsinki, Moscow, Bremen, Uppsala...

People worked/working on graphene in our group:

Misha Akhukov, Danil Boukhvalov, Annalisa Fasolino, Jan Los, Koen Reijnders, Rafa Roldan, Sasha Rudenko, Guus Slotman, Misha Titov, Timur Tudorovskiy, Merel van Wijk, Shengjun Yuan, Kostya Zalharchenko

Special thanks also to Andre Geim, Kostya Novoselov, Paco Guinea, Sasha Lichtenstein, Tim Wehling...

Impossible to mention everyone...